PCP
PLANT & CELL PHYSIOLOGY

Regular Paper

Laser Microdissection Coupled to Transcriptional Profiling of Arabidopsis Roots Inoculated by *Plasmodiophora brassicae* Indicates a Role for Brassinosteroids in Clubroot Formation

Astrid Schuller[1,3], Julia Kehr[2] and Jutta Ludwig-Müller[1,*]

[1]Institut für Botanik, Technische Universität Dresden, D-01062 Dresden, Germany
[2]Molekulare Pflanzengenetik, Biozentrum Klein Flottbek, D-22609 Hamburg, Germany
[3]Present address: Institut für Genetik, Technische Universität Dresden, D-01062 Dresden, Germany.
*Corresponding author: E-mail, Jutta.Ludwig-Mueller@tu-dresden.de; Fax, +49-351-463-37032.
(Received April 23, 2013; Accepted November 20, 2013)

The clubroot disease caused by the obligate biotrophic protist *Plasmodiophora brassicae* on host plants of the Brassicaceae family is characterized by enhanced cell division and cell expansion. Since a typical root section of an infected plant always includes different stages of the pathogen as well as uninfected cells, we were interested in investigating specific developmental stages of the pathogen and their effect on host transcriptional changes. We extended previous microarray studies on whole roots by using laser microdissection and pressure catapulting (LMPC) to isolate individual cells harboring defined developmental stages of the pathogen. In addition, we compared the central cylinder of infected plants with that of control plants. We were especially interested in elucidating the stage-specific hormonal network. The up-regulation of genes involved in auxin and cytokinin metabolism and signaling was confirmed. In addition, we found evidence that brassinosteroid (BR) synthesis and signal perception genes were in many cases up-regulated in enlarged cells and the central cylinder. This was confirmed by quantitative PCR. Treatment of wild-type plants with the BR biosynthesis inhibitor propiconazole reduced gall formation, and the analysis of the BR receptor mutant *bri1-6* revealed less severe gall formation than in the respective wild type. Our results identify novel hormone pathways involved in clubroot development. Using LMPC to generate pools of homogeneous cell type populations combined with transcriptome analysis has been very useful to elucidate the regulation of gall growth by this obligate biotropic pathogen in a cell- and stage-specific manner.

Keywords: *Arabidopsis thaliana* • Brassinosteroid • Clubroot disease • Homogeneous cell type populations • LMPC • *Plasmodiophora brassicae* • Propiconazole • Transcriptome.

Abbreviations: ARF, auxin response factor; BR, brassinosteroid; CC, central cylinder; dai; days after inoculation; DI, disease index; ET, ethylene; JA, jasmonate; LMPC, laser microdissection and pressure catapulting; LP, large plasmodia; PP2A, protein phosphatase 2A; RT–PCR, reverse transcription–PCR; SP, small plasmodia; TCA, tricarboxylic acid.

Introduction

Plants within the family Brassicaceae are subject to infection with the obligate biotrophic protist *Plasmodiophora brassicae*. Using *Arabidopsis thaliana* as a model system has allowed the application of available genetic and molecular tools and has thus advanced our knowledge of this economically important plant disease (Siemens et al. 2002). The plant hormones auxin and cytokinin play a role during gall formation, inducing hypertrophy and hyperplasia by increased cell division rates and cell enlargement (Ludwig-Müller and Schuller 2008, Ludwig-Müller et al. 2009). When host roots have been transformed into galls, the nutrition of the pathogen is dependent on sugar translocation from the host plant (Siemens et al. 2011). The investigation of Arabidopsis mutants involved in various metabolic pathways has provided only limited insight into the mechanisms by which the parasite can change the host metabolism (Siemens et al. 2002, Alix et al. 2007). Therefore, several '-omics' studies on the two different phases of the *P. brassicae* life cycle have been performed. The first phase comprises the colonization of host root hairs, while the secondary phase is confined to the cortex of the roots (Kageyama and Asano 2009). Transcriptome analyses during the root hair infection phase preceding the infection of the cortex showed only a small number of genes altered in expression (Agarwal et al. 2011). In contrast, comparisons of the transcriptome during two time points of the secondary infection phase of the root cortex revealed a high number of up- or down-regulated genes (Siemens et al. 2006). Proteome data from Arabidopsis and *Brassica* roots infected with *P. brassicae* gave indications for additional proteins possibly involved in the interaction (Devos et al. 2005, Cao et al. 2007). Technically, the problem is that an infected root is a mixture of different cell types harboring different

Plant Cell Physiol. 55(2): 392–411 (2014) doi:10.1093/pcp/pct174, available online at www.pcp.oxfordjournals.org

developmental stages of the pathogen. In the beginning of the secondary infection, myxamoebae of the pathogen are observed (Kobelt 2000). Later plasmodia develop and grow first in the vicinity of the vascular bundle; afterwards they can be found in the outer cortex close to the rhizodermis. These multinucleate plasmodia eventually form resting spores (Ludwig-Müller and Schuller 2008), destroying the structure of the host cell. Therefore, it is necessary to analyze the global gene expression patterns in more detail in a cell type-specific manner.

Different methods can be used for analysis of individual cells or groups of cells belonging to a certain cell type. The method of choice, even though technically demanding, is laser microdissection (LM), by which individual cells are cut out, pooled and finally analyzed. Recently, this method has been successfully used in plant–microbe interactions for arbuscular mycorrhiza symbiosis (Guether et al. 2009, Gaude et al. 2012), powdery mildew infection of Arabidopsis (Chandran et al. 2010), as well as the interaction of host plants with parasitic nematodes (Klink et al. 2005, Klink et al. 2009). Alternatively, syncytia induced in Arabidopis roots by *Heterodera schachtii* were transcriptionally analyzed by using microaspiration (Szakasits et al. 2009). This method would be difficult to use for the root galls induced by *P. brassicae* due to their thickness. Even though the methods for LM have been described in several papers (e.g. Thome et al. 2006, Deeken et al. 2008, in addition to those mentioned above), they are still not routinely applied. Therefore, many methodological improvements and adaptations to a given plant material need to be carried out.

While the growth hormones auxin and cytokinin have been studied during clubroot development, not much evidence for the involvement of other growth-promoting hormones in the induction of club growth has been presented. For gibberellins, several genes were reported to be up-regulated in a microarray study (Siemens et al. 2006), but treatment of *P. brassicae*-infected Arabidopsis plants with an inhibitor of gibberellin biosynthesis did not result in reduced gall size (Päsold and Ludwig-Müller 2013), making a contribution of gibberellins to clubroot development unlikely. Evidence for the involvement of brassinosteroids (BRs) has been obtained from mutant analysis (Siemens et al. 2002). The *det2* mutation resulted in less severe galls, even though the plants are dwarfed. DET2 is involved in the biosynthesis of BR (Li et al. 1997).

In general, BRs are involved in such diverse processes as cell elongation, cell division, senescence, vascular differentiation, reproduction, photomorphogenesis and responses to various stresses (reviewed in Ye et al. 2011). BR function in several of these processes overlaps with that of auxin, but defects cannot be completely complemented by the other respective hormone. The biosynthetic pathway of BR is complex and involves several alternative branches (Fujioka and Yokota 2003). The perception of the signal is dependent on the plasma membrane-bound receptor kinase BRI1 (Clouse 2011a, Ye et al. 2011). The involvement of additional receptor-like kinases, such as BAK1, in the BR response suggests that the receptors might interact with each other and are functional only as oligomers (Clouse 2011a). Further downstream, a kinase named BIN2 phosphorylates the transcription factors BES1 and BZR1, thereby converting these into an inactive state. Activation of these transcription factors is achieved by the activity of a phosphatase [protein phosphatase 2A (PP2A); Clouse 2011a]. Dephosphorylated BES1 and BZR1 activate BR-responsive genes alone or together with accessory transcription regulators, resulting in transcriptional networks. Further proteins associated with the regulation of this pathway have been discovered recently (Ye et al. 2011).

Since BR also interacts with auxin at different levels (Halliday 2004), it was of interest to determine whether BR is an additional factor controlling gall size after infection with *P. brassicae*. In a microarray performed on whole root tissue infected with *P. brassicae* that was compared with whole control roots, an involvement of BR in gall formation was not evident (Siemens et al. 2006). The present study has used LMPC for the first time to isolate individual cells harboring defined developmental stages of the pathogen in this intricate plant–pathogen interaction. This work demonstrates plasmodial stage-specific transcriptional changes of the host cells. In addition, the tissues representing the central cylinders of control and infected roots were compared. Here, we present evidence that BR synthesis and signaling are involved in gall size, which was confirmed using the BR synthesis inhibitor propiconazole (Hartwig et al. 2012) and the BR receptor mutant *bri1-6*. In addition, the analysis of the total transcriptome of homogeneous cell type populations of Arabidopsis harboring various stages of plasmodia, the major developmental form of *P. brassicae* in the host root, led to the identification of other metabolic pathways, which could play a role in clubroot development.

Results

Single cells with different plasmodial stages can be isolated from *Plasmodiophora brassicae*-infected Arabidopsis roots

A major problem when dealing with plant–pathogen interaction occurs due to a mixture of infected and non-infected cells within a given tissue, especially with obligate biotrophic pathogens such as *P. brassicae*, the causal agent of clubroot disease. In addition, the developmental stages of the pathogen cannot be synchronized, so that small and large plasmodia occur simultaneously (**Fig. 1A, B**), and, during later stages, which were not analyzed here, resting spores are also present in the same root section. We therefore hypothesized that the analysis of homogeneous cell type populations harboring different states of the pathogen could contribute to solving this problem.

We used LMPC with sections of paraffin-embedded Arabidopsis roots infected with *P. brassicae* and control roots

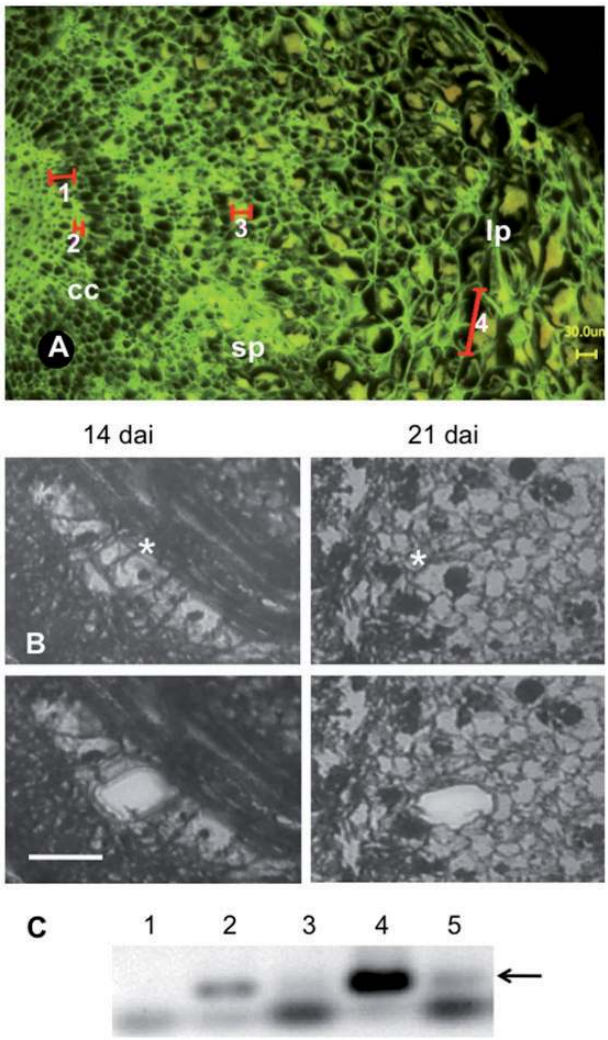

Fig. 1 Using laser microdissection and pressure catapulting (LMPC), it is possible to isolate single cells harboring the clubroot pathogen *Plasmodiophora brassicae*. (A) Example of a cross-section used for the different experiments under fluorescent light. cc, central cylinder; sp, small plasmodia; lp, large plasmodia. With the red bars, the size is indicated for 1, 31.46 μm; 2, 10.66 μm; 3, 28.57 μm; and 4, 91.04 μm. (B) Pictures from sections 14 days after inoculation (dai) and 21 dai, where the cell type used for LMPC is indicated by an asterisk. Left column images show a longitudinal section; right column images a cross-section. The second panel shows the same section after catapulting out the single cell. The scale bar represents 10 μm. (C) RT–PCR experiment with RNA isolated from either embedded or LMPC-collected samples and detection of *P. brassicae* actin transcripts. Lane 1, non-infected root (34 d after germination); lane 2, infected root (pooled sample at different days after inoculation); lane 3, paraffin-embedded LMPC-isolated host control cells (same age as sample 5); lane 4, paraffin sections of complete infected root section 24 dai; lane 5, paraffin-embedded LMPC-isolated host cells containing large plasmodia (24 dai). The actin band is marked by an arrow; below are primer dimers.

to isolate individual cells harboring defined developmental stages of the pathogen and the complete central cylinder. LMPC was successfully performed (**Fig. 1B**). Using 20 μm thick longitudinal and cross-sections of paraffin-embedded 14- and 21-day-old infected roots, small plasmodia-containing cells close to the central stele (left column) and large plasmodia-containing cells in the root cortex (right column) could have been isolated, as well as the complete central cylinder (not shown). A section thickness of 20 μm was chosen due to the enlargement of the hypertrophied cells. To verify that RNA could be obtained and reverse transcription–PCR (RT–PCR) fragments could be amplified from isolated cells, initial investigations were performed. In addition to the complex tissues of infected and control roots and sections of embedded infected roots we used LMPC-sampled individual control cells and cells harboring plasmodia. A *P. brassicae* transcript (*PbActin*) of 135 bp could only be detected in infected roots and large plasmodia-containing cells (**Fig. 1C**, arrow).

For subsequent microarray hybridizations, cell sampling was done with 20 μm cross-and longitudinal sections of 14- and 21-day-old infected and control roots. The following samples were used for comparison (**Fig. 2A**, **Table 1**): a control which was the total root section without the central cylinder (14c), the central cylinder only from control roots (14cc), the central cylinder only from infected roots (14cci), host cells with small plasmodia close to the central cylinder (14sp), hypertrophied host cells with large plasmodia in the cortex area (14lp) and, from 21 days after inoculation (dai) and respective controls, a control which was the total root section without the central cylinder (21c), infected host cells close to the central cylinder (21sp) and hypertrophied host cells with large plasmodia in the cortex area (21lp). In general there exist several options to define the control material: (i) individual healthy cells from control tissue; (ii) individual non-infected cells from an infected root section; and (iii) complete sections of control roots treated as the infected sections prior to LMPC. The latter was chosen to prevent too high variation at least in the control samples. The comparison of the central cylinder of infected and control plants was performed because (i) *P. brassicae* was found in the xylem of infected plants (Ludwig-Müller et al. 1999) and (ii) the vasculature could serve as an exchange point for signals and nutrients between roots and leaves of the plant, e.g. transport of nutrients to *P. brassicae* and signals to distant tissues.

The homogeneous cell type populations generated by LMPC consisted of 345 (14sp), 293 (14lp), 364 (21sp) and 429 (21lp) cells, respectively. The mean cell size in the different samples corresponded to the increased hypertrophy of infected cells harboring large plasmodia (**Supplementary Fig. S1**). In **Fig. 1A** a scale for a non-infected cell, small and large plasmodia is also indicated. Differential transcriptional responses were evaluated and analyzed in detail for the following samples (**Table 1**): 14cci vs. 14cc (14CC), 14sp vs. 14c (14SP), 14lp vs. 14c (14LP), 21sp vs. 21c (21SP) and 21lp vs. 21c (21LP), with a 2-fold up- or down-regulation as cut-off. We will concentrate in the following on the results of these five ratios. Comparison of

all differentially regulated genes in these ratios revealed that the highest number was found for both samples with large plasmodia (14LP, which are still differentiating and 21LP, which are mostly differentiated). There were almost similar numbers of transcripts up- or down-regulated in the different stages (Fig. 2B).

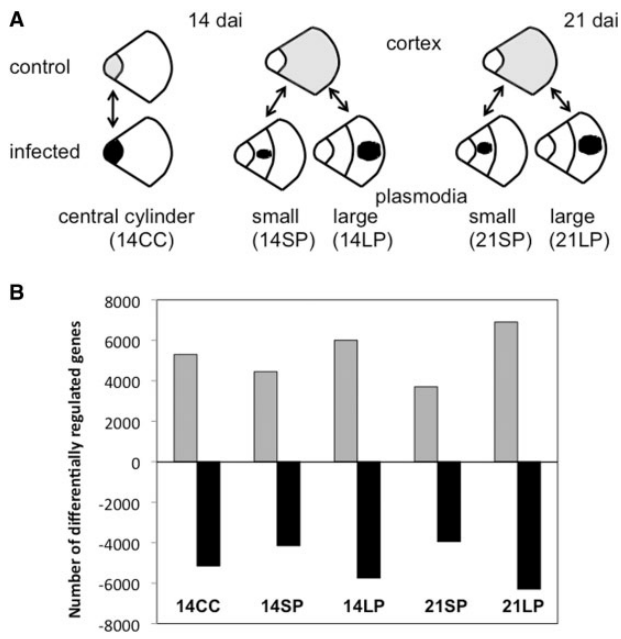

Fig. 2 Description of the samples used for this study (see also **Table 1** for more details). (A) The cartoons show the different comparisons and locations of the samples within the section in gray (control) and black (infected); dai, days after inoculation. For more details on the different comparisons see text and **Table 1**. (B) Number of genes differentially regulated after microarray analysis. The samples were 14CC (central cylinder infected vs. control 14 dai), 14SP (cells with small plasmodia vs. control cortex 14 dai), 14LP (cells with large plasmodia vs. control cortex 14 dai), 21SP (cells with small plasmodia vs. control cortex 21 dai) and 21LP (cells with large plasmodia vs. control cortex 21 dai). Cut-off for differential regulation was ≤ -2 or ≥ 2.

Differential gene expression in major metabolic pathways

To get an impression of the general transcriptional changes in major metabolic pathways, the data were processed and displayed using MapMan (Thimm et al. 2004, **Fig. 3**). Genes indicated in blue in the figure showed an up-regulation and those in red were down-regulated. Infection per se correlated in most samples with higher metabolic activities, such as major carbohydrate synthesis (starch, sucrose and glycolysis), the tricarboxylic acid (TCA) cycle and lipid metabolism. With respect to metabolic changes, the major differences could be observed between small and large plasmodia and less between the different time points. On the other hand, general cell wall metabolism was down-regulated in these large hypertrophied cells. In small cells from 14- and 21-day-old roots harboring small plasmodia, MapMan analysis indicated some induction of metabolic pathways, especially in the categories tetrapyrrole, light reaction, N and S metabolism, glycolysis, TCA cycle and fermentation (for an overview of all pathways see **Supplementary Fig. S2**). In large plasmodia-containing cells from 14- and 21-day-old roots (14LP and 21LP) the induction of the same metabolic pathways was much stronger, an indication for plasmodia with high metabolic activity (**Fig. 3**). In line with these observations, the comparison between infected and control central cylinders (14CC) also showed not so much metabolic activity, comparable with 14SP. With respect to metabolic pathways, the infected root can be viewed as having concentric layers with different activities, first the central cylinder, then the inner cortex layer surrounding the central cylinder with mainly small plasmodia, and finally the outer cortex layer with large plasmodia.

With regard to synthesis of secondary metabolites (**Supplementary Fig. S3**), the differential regulation of terpene

Table 1 Description of LMPC samples used for transcriptional analysis

Sample name	Description	Comparison in microarray
14cc	Central cylinder from control roots 14 d after inoculation	
14cci	Central cylinder from infected roots 14 d after inoculation	14CC = 14cci vs. 14cc (infected central cylinder 14 dai vs. control central cylinder 14 dai)
14c	Cortex from control roots 14 d after inoculation	
14sp	Host cells with small plasmodia close to the central cylinder 14 d after inoculation	14SP = 14sp vs. 14c (infected cell 14 dai vs. control cortex 14 dai)
14lp	Hypertrophied host cells with large plasmodia in the cortex area 14 d after inoculation	14LP = 14lp vs. 14c (infected cell 14 dai vs. control cortex 14 dai)
21c	Cortex from control roots 21 d after inoculation	
21sp	Host cells with small plasmodia close to the central cylinder 21 d after inoculation	21SP = 21sp vs. 21c (infected cell 21 dai vs. control cortex 21 dai)
21lp	Hypertrophied host cells with large plasmodia in the cortex area 21 d after inoculation	12LP = 21lp vs. 21c (infected cell 21 dai vs. control cortex 21 dai)

dai, days after inoculation; control roots were the same age.
For a graphical depiction of sample details see **Fig. 2**.

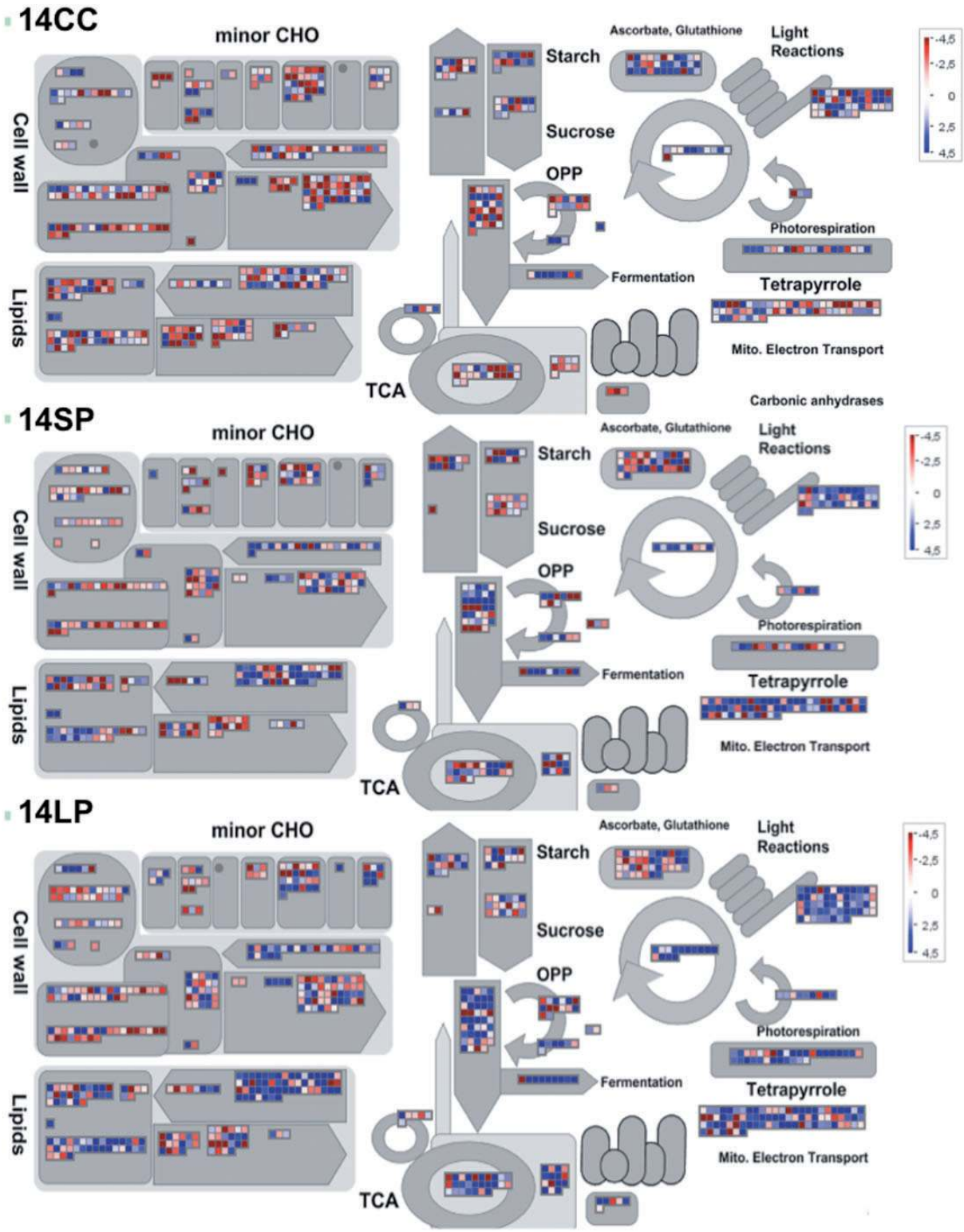

Fig. 3 MapMan analysis for metabolism. Only a part of the metabolic overview is shown here; the complete data set is shown in **Supplementary Fig. S2**. The samples were 14CC (central cylinder infected vs. control 14 dai), 14SP (cells with small plasmodia vs. control cortex 14 dai), 14LP (cells with large plasmodia vs. control cortex 14 dai), 21SP (cells with small plasmodia vs. control cortex 21 dai) and 21LP (cells with large plasmodia vs. control cortex 21 dai). For detailed sample description, see **Fig. 2** and **Table 1**. Blue, up-regulated; red, down-regulated.

(continued)

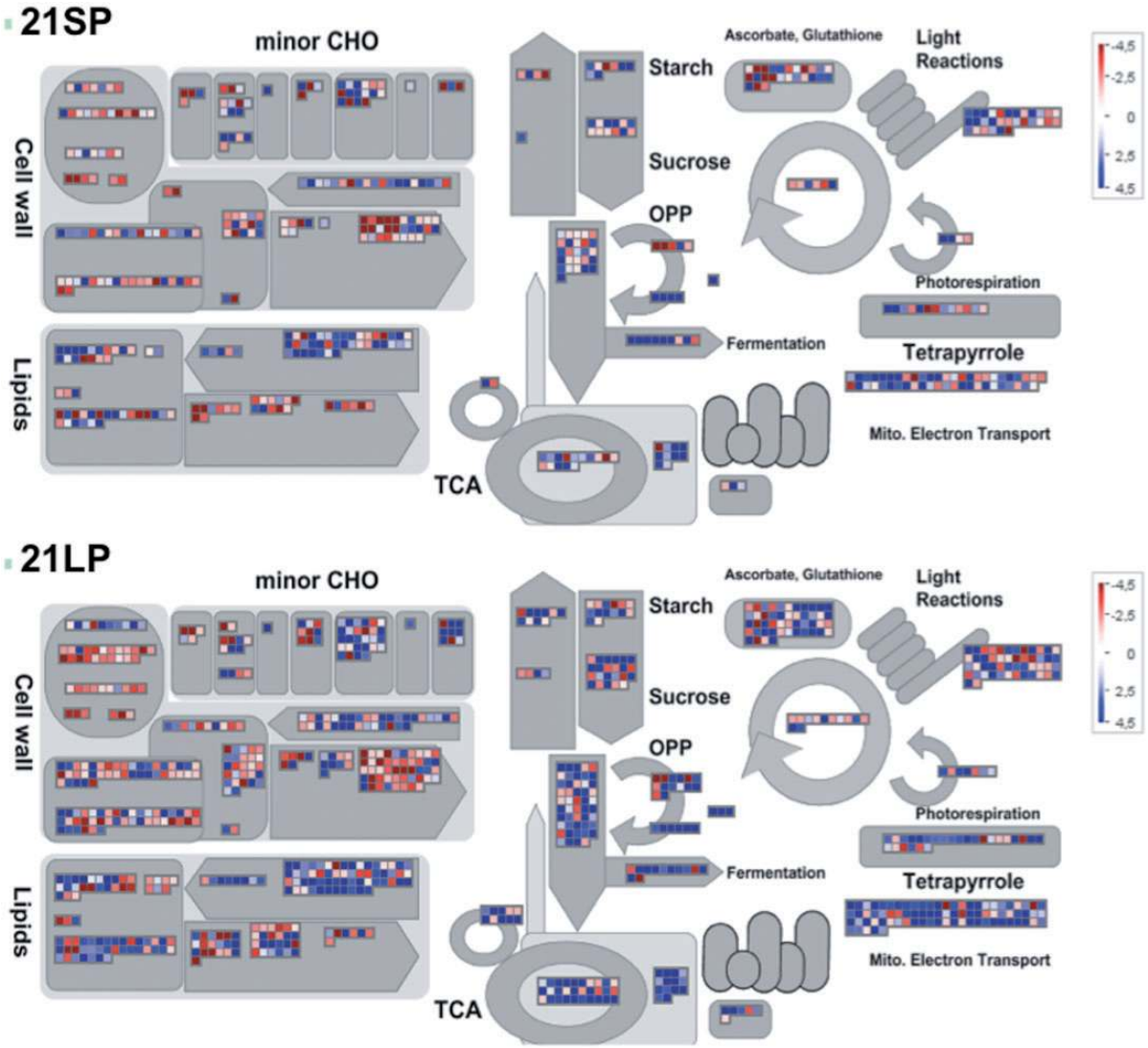

Fig. 3 Continued.

biosynthesis is interesting to note. In all ratios from plasmodia-containing cortex cells the genes from the non-mevalonate pathway were mostly down-regulated, while those from the mevalonate pathway were up-regulated. In the central cylinder, the regulation was just the opposite, even though transcriptional changes were not so prominent. There was an up-regulation of the shikimate pathway and flavonoid synthesis in cells harboring large plasmodia at 14 dai and especially at 21 dai, while anthocyanins are regulated in the opposite manner. Other secondary metabolite pathways, including that of defense compounds such as glucosinolates, did not show a clear regulation pattern in any of the comparisons (**Supplementary Fig. S3**).

While MapMan displays gene expression data from a single comparison of two conditions, PageMan (Usadel et al. 2005) analyzes data series from time courses and/or treatments. One problem with these types of data sets is usually that due to the sheer number of data points it is difficult to visualize an overview of the data. PageMan can display several experiments in parallel and can thereby indicate the changed number of transcripts for a certain process. This gives a cluster of gene families regulated similarly in the different comparisons. Further analysis using the GO (Gene Ontology) terms within PageMan showed that fermentative processes and lipid synthesis in particular were up-regulated in cells with plasmodia (**Supplementary Fig. S4**). In contrast, β-oxidation and other lipid degradation processes were down-regulated, which may be an indication for lipids as storage products of *P. brassicae* (Ikegami et al. 1982).

Plant defense-associated hormones

Hormones involved in plant defense responses, such as jasmonate (JA) and ethylene (ET), were also differentially regulated at the cellular level. For JA synthesis (**Supplementary Fig. S5**), mostly increased transcript amounts were observed for all

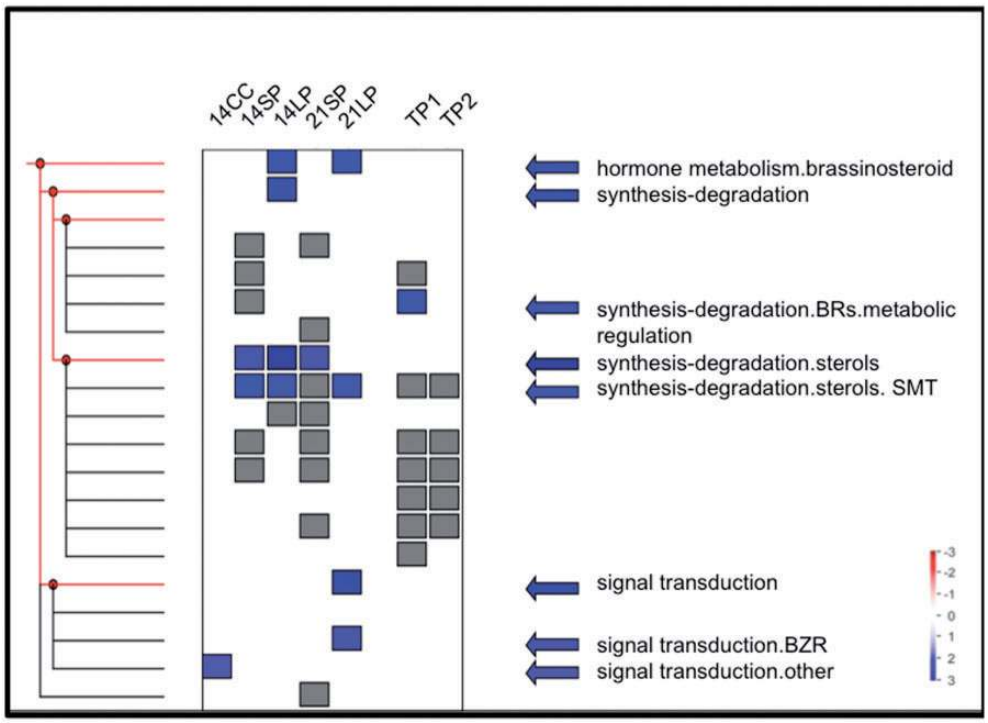

Fig. 4 PageMan analysis for brassinosteroids (BRs). Here the data from the whole root microarray (Siemens et al. 2006) are also included. TP1, 10 dai of whole root microarray; TP2, 23 dai of whole root microarray. The samples from the homogeneous cell sample array were 14CC (central cylinder infected vs. control 14 dai), 14SP (cells with small plasmodia vs. control cortex 14 dai), 14LP (cells with large plasmodia vs. control cortex 14 dai), 21SP (cells with small plasmodia vs. control cortex 21 dai) and 21LP (cells with large plasmodia vs. control cortex 21 dai). For detailed sample description, see **Fig. 2** and **Table 1**. Blue, up-regulation; gray, items that are flagged as being unreliably measured.

investigated root cells harboring different developmental stages of *P. brassicae*. Also, the JA signaling pathway was differentially regulated. A down-regulation of the signaling components *JAR1* [synthesis of the receptor ligand jasmonyl-isoleucine (JA-Ile)] and *COI1* (receptor) specifically in the central cylinder was observed, while three *JAZ* transcriptional repressor genes were actually up-regulated (**Supplementary Table S4**). Cells with older plasmodia, and especially large plasmodia from 21-day-old roots (21LP), showed elevated transcription of ET synthesis genes (**Supplementary Fig. S5**), as indicated by the more reddish colors, while ET synthesis in cells harboring younger plasmodia was not as clearly regulated. Salicylic acid and ABA metabolism and signaling were down-regulated in large plasmodia-containing cells 14 dai (data not shown).

Plant growth-promoting hormones

Plant hormones, especially auxins and cytokinins, are important to clubroot development (see comparisons with whole root array data in the **Supplementary tables**). The GH3 family IAA–amino acid conjugate synthetases (**Supplementary Table S1**) and also IAA–amino acid conjugate hydrolases (**Supplementary Fig. S6**) were differentially expressed in plasmodia-containing cells, indicating highly active auxin metabolism. A gene from the nitrilase family involved in auxin synthesis, *Nitrilase2* (*Nit2*), was up-regulated in large plasmodia-containing cells from 14- and 21-day-old roots (14LP and 21LP) (**Supplementary Fig. S6**, **Supplementary Table S1**). Also another auxin biosynthesis gene, *CYP79B2*, is up-regulated in these samples, but the homologous gene *CYP79B3* is down-regulated (14SP, 14LP and 21SP) as shown in the AraCyc pathways (**Supplementary Fig. S6**). Root-specific cytokinin oxidase *CKX1* and *CKX6* genes were down-regulated in complete root gall tissues compared with controls (Siemens et al. 2006), whereas *CKX4* was up-regulated at the late time point of infection. The LMPC analysis could confirm the down-regulation of *CKX1* for the infected central cylinder and especially for cells containing large plasmodia (**Supplementary Table S2**). In addition, down-regulation of *CKX3* and *CKX7* in the infected central cylinder and of *CKX3* also in large plasmodia-containing cells has been observed. A different expression pattern for *CKX6* was observed with LMPC samples. *CKX6* was down-regulated only in the infected central cylinder and was strongly up-regulated in plasmodia-containing cells of the cortex.

Brassinosteroid-related transcripts are differentially regulated

In this work we could identify several components in BR synthesis and signaling, which are differentially regulated in root cells harboring different developmental stages of *P. brassicae* (**Figs. 4–6**; **Table 2**; **Supplementary Table S3**). The PageMan

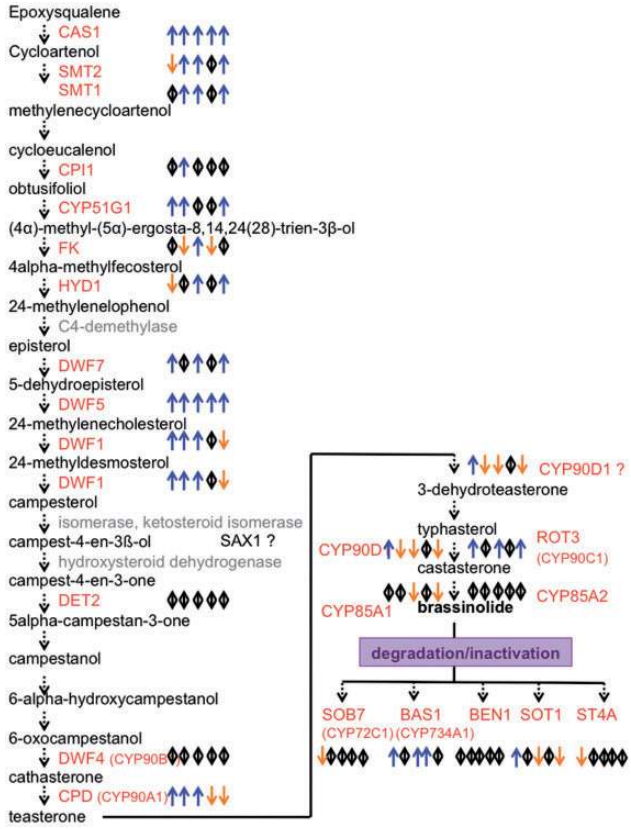

Fig. 5 Differential regulation of brassinosteroid biosynthesis taken from AraCyc (www.arabidopsis.org). Only one biosynthesis branch is shown. The last branch contains enzymes involved in the inactivation. Samples are given in the following order: 14CC, 14SP, 14LP, 21SP and 21LP. For details, see the legend of **Fig. 3**, **Table 1** and text. Blue arrow, up-regulation; orange arrow, down-regulation; black arrow, no regulation. Abbreviations for enzymes are given in red, those where no further information is available in gray and those of compounds in black.

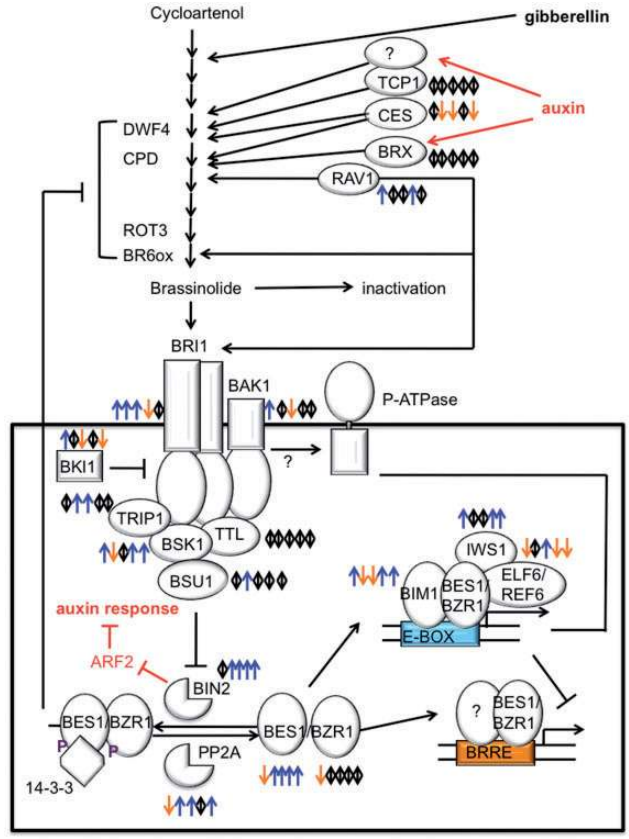

Fig. 6 Differential regulation of brassinosteroid biosynthesis by putative transcription factors (upper part of figure) and signaling (lower part of figure) redrawn according to Ye et al. (2011). Samples are given in the following order: 14CC, 14SP, 14LP, 21SP and 21LP. For details, see the legend of **Fig. 3**, **Table 1** and text. Blue arrow, up-regulation; orange arrow, down-regulation; black arrow, no regulation. For details on the regulation of synthesis and metabolism, see **Fig. 5**. Phosphorylation of BEZ1/BZR1 results in protein degradation, cytoplasmic retention and reduced DNA binding, and also has an inhibitory effect on some biosynthesis steps. Activation of BR-responsive genes results in various features, i.e. cell elongation, cell division, root growth, xylem development and stress responses. The interactions with respect to auxin are shown in red.

overview (**Fig. 4**) indicates a significant up-regulation of BR metabolism for hypertrophied cells, i.e. cells with large plasmodia at both time points, 14LP and 21LP, as well as enhanced signal transduction in cells with large plasmodia, 21LP. The central cylinder exhibited clear transcriptional activation only for signal transduction, while the 21SP sample only showed strong regulation in the category synthesis–degradation. A more detailed analysis of the pathways revealed that most transcripts encoding components of the biosynthetic pathway were up-regulated (**Fig. 5**; **Supplementary Table S3**). For example, transcripts encoding *CAS1* and *DWF5* were increased in all samples, whereas other genes were confined in their regulation to some plasmodial stages. It should be noted that the expression of some genes of the BR synthesis pathway was also increased in the central cylinder of infected plants. In contrast, genes encoding enzymes for BR metabolism and degradation were either down-regulated or not regulated at all in the investigated LMPC samples. The only exception was *BAS1* that was up-regulated in the central cylinder and in 14LP and 21SP. Interestingly, transcription of this gene was also strongly up-regulated in the whole root array at TP1.

While transcription factors possibly controlling BR biosynthetic genes were not considerably regulated (**Fig. 6**), components of the signaling pathway were more often up-regulated (**Fig. 6**; **Table 2**). The data for genes involved in BR signal transduction were compiled from Ye et al. (2011) and Clouse (2011b). The gene encoding the membrane-bound leucine-rich repeat receptor-like kinase *BRI1*, required for BR perception, was strongly up-regulated in 14CC, 14SP and 14LP cells. In agreement with this, this gene was also up-regulated at 10 dai in the whole root array, even though with a small induction rate of 2-fold. *BKI1*, a membrane-associated negative regulator of BR signaling that in the absence of BR probably prevents binding of

Table 2 Differential regulation of selected brassinosteroid signaling-associated genes

AGI No.	Gene name	Array result whole root		Array result LMPC samples				
		TP1	TP2	14CC	14SP	14LP	21SP	21LP
At4g39400	*BRI1*	2.05	0	11.85	55.55	55.58	−100	0
At2g01950	*BRL2*	3.14	−4.17	−12.80	17.35	0	−100	−9.59
At3g13380	*BRL3*	0	0	−22.48	−100	−100	0	21.71
At5g42750	*BKI1*	0	5.29	2.08	0	−3.96	0	−6.23
At4g33430	*BAK1*	0	0	62.54	0	−2.55	0	0
At2g46280	*TRIP1*	0	0	0	49.71	64.39	0	0
At5g58220	*TTL*	0	2.02	0	0	0	0	0
At4g35230	*BSK1*	0	0	3.23	−25.32	0	4.60	15.09
At5g46570	*BSK2*	3.80	0	0	15.90	27.21	0	8.32
At4g00710	*BSK3*	0	0	−6.32	−11.68	−2.37	0	6.04
At1g03445	*BSU1*	0	0	0	8.17	0	0	0
At4g18710	*BIN2*	−2.70	0	0	11.77	52.73	100	99.41
At1g06390	*BIL2*	0	2.41	0	−15.48	−5.46	15.49	65.53
At1g19350	*BES1*	Nt on Affymetrix array		−2.24	2.41	8.56	8.76	100
At1g75080	*BZR1-1*	0	0	−27.01	0	0	0	0
At3g50750	*BEH1*	−2.70	4.01	0	−4.33	−8.79	0	−4.89
At1g69960	*PP2A*	0	0	−5.46	100	100	0	80.09
At5g08130	*BIM1*	2.27	2.61	2.41	−2.15	−2.12	100	100
At5g04240	*ELF6/REF6*	0	0	−2.95	0	2.42	−100	−100
At1g32130	*IWS1*	0	0	2.75	0	0	100	5.68
At4g30610	*BRS1*	0	0	100	0	0	0	0
At1g71930	*VND7*	−2.04	0	−45.04	−3.33	−3.05	0	−3.90
At5g62380	*VND6*	0	−4.76	−8.82	−11.24	−3.03	0	−3.32

A larger compilation can be found in **Supplementary Table S3**.
Transcripts were considered up- or down-regulated at ≥ 2-fold induction/repression. For simplification, values below this threshold are given as '0' regulation.
The two time points for the whole root Affymetrix microarray were TP1 10 days after inoculation (dai) and TP2 23 dai (Siemens et al. 2006).
The samples from the Agilent array using LMCP samples were 14CC (central cylinder infected vs. control 14 dai), 14SP (cells with small plasmodia compared with control cortex 14 dai), 14LP (same for cells with large plasmodia), 21SP (cells with small plasmodia compared with control cortex 21 dai) and 21LP (same for large plasmodia).
Up-regulated genes are marked in blue, and down-regulated genes in orange. 100/−100 is the cut-off for up-regulation and means that the regulation is equal to or larger than this value.

the BRI1 co-receptor BAK1, was up-regulated in 14CC and down-regulated in 14LP and 21LP. *BAK1* itself, which stimulates BRI1 kinase activity, was strongly up-regulated in 14CC. *TRIP1*, another putative cytoplasmic substrate of BRI1, was strongly up-regulated in 14SP and 14LP. Positive regulators of BR signaling, such as the BRI1 interactors *BSK1*–*BSK3*, were differentially regulated in the investigated tissues and cell types. In response to BR, BRI1 phosphorylates BSK1 and phosphorylated BSK1 interacts with the phosphatase BSU1 and by this promotes its interaction with the negative regulator BIN2, which plays a central role in the downstream signaling process. BSU1 dephosphorylates BIN2, resulting in its inactivation. BIN2 negatively regulates BR signaling by phosphorylating the transcription factors BZR1 and BES1. Phosphorylation of BZR1 and BES1 inhibits their DNA binding ability and dimerization with other transcription factors. *BSU* transcripts were only up-regulated in 14SP. On the other hand, a strong up-regulation of *BIN2* was observed in all infected cortex cells at both time points. The up-regulation of *BIN2* could also indicate an induction of auxin-mediated gene expression, because BIN2 phosphorylation prevents binding of the repressor auxin response factor 2 (ARF2) to the promoter of auxin-responsive genes (Vert et al. 2008). In the same plasmodia-containing samples, the transcription factor *BES1* was also strongly up-regulated. Interestingly, *BIN2* was not regulated in the central cylinder, in contrast to the transcription factors *BZR1-1* and *BES1*, which were both down-regulated in the central cylinder. PP2A is involved not only in dephosphorylation and thereby in activation of the transcription factors BZR1 and BES1, but also in degradation of BRI1 (Ye et al. 2011). The *PP2A* transcript was down-regulated only in 14CC, but it was strongly up-regulated in 14SP, 14LP and 21LP.

In response to BR activation, BZR1 and BES1 bind to the promoters of hundreds of BR-responsive genes, whereas they can act as both transcriptional activators and repressors. Dimerization/interacting partners have been reported, such

Table 3 Verification of transcriptome data by quantitative RT–PCR for selected genes in BR biosynthesis and signaling

AGI	Gene name		14CC	14SP	14LP	21SP	21LP
At3g19820	*DWF1*	Array	2.40	19.40	100.00	0.00	−52.67
		qPCR	2.07	Up	Up	100.00	59.63
At1g50430	*DWF5*	Array	20.00	6.90	57.51	100.00	71.86
		qPCR	5.12	100.00	100.00	Up	Up
At4g39400	*BRI1*	Array	11.85	55.55	55.58	−100.00	0.00
		qPCR	19.85	100.00	100.00	−100.00	−4.29
At5g08130	*BIM1*	Array	2.41	−2.15	−2.12	100.00	100.00
		qPCR	4.06	Up	Up	Up	Up

The samples were 14CC (central cylinder infected vs. control 14 dai), 14SP (cells with small plasmodia compared with control cortex 14 dai), 14LP (same for cells with large plasmodia), 21SP (cells with small plasmodia compared with control cortex 21 dai) and 21LP (same for large plasmodia).
For some control samples, no PCR product was obtained, but the sample from infected tissue gave values. In these cases, the regulation was designated 'Up'. As a cut-off for differential regulation, a value of 100 (as in the microarray data) is given.

as BIM1, ELF6/REF6 and transcription elongation factor IWS1. *BIM1* was slightly up-regulated in 14CC and strongly up-regulated in 21SP and 21LP. On the other hand, a slight down-regulation was observed for 14SP and 14LP. *IWS* was also slightly up-regulated in 14CC, and more strongly up-regulated in 21SP and 21LP. *ELF6/REF6* showed an opposite regulation. Other downstream factors involved in signaling are the NAC-domain transcription factors VND6 and VND7, whose transcripts showed strong down-regulation in all samples, with the exception of 21SP (**Table 2**). Lastly, the gene *BRS1*, encoding a carboxypeptidase, which was isolated as a repressor of BRI1, was strongly up-regulated in the central cylinder. Further evidence for its function was provided by the investigation of gall formation of mutant lines (**Fig. 8**).

To verify the transcriptome data by quantitative RT–PCR, we chose several genes from the BR biosynthesis and signaling pathways (**Table 3**), as well as genes annotated to different hormone pathways and one gene from primary metabolism (**Supplementary Table S4**). The up-regulation of *DWF5*, a gene encoding an enzyme of the biosynthetic pathway, was confirmed in all individual cell samples. The regulation of *DWF1* was confirmed in three of the five samples. The expression patterns for all homogeneous cell type samples were also confirmed for the receptor gene *BRI1* and in three samples (14CC, 21SP and 21LP) for *BIM1*. Thus, we could verify approximately 75% of the microarray data by additional qRT–PCR, which is in the range of published confirmations of these kinds of experiments (e.g. Bruder et al. 2007; verification of nine out of 12 samples by quantitative PCR). For several other genes not belonging to the BR pathway, we could also verify the gene expression patterns by quantitative RT–PCR (**Supplementary Table S4**) as shown for the central cylinder (14CC). Here, the results showed an even higher percentage of verification, as 14 out of 15 data sets could be confirmed. For certain genes, no PCR products in the quantitative RT–PCR experiments were obtained in the control samples, most probably because the expression levels were at the detection limit. In these cases, the regulation was designated 'up'. Variations in transcription levels between microarrays and quantitative PCR have already been described (Morey et al. 2006).

Impairment of brassinosteroid biosynthesis and signaling results in tolerance to the clubroot disease

To confirm the results that have been obtained by microarray analysis following LMPC of infected host cells indicating a role for BR synthesis and signaling in clubroot development, we investigated the effect of (i) a BR biosynthesis inhibitor and (ii) mutations in BR signaling components on clubroot development. As an inhibitor of BR synthesis, the recently introduced propiconazole was tested (Hartwig et al. 2012). The treatment started with the time point of inoculation, so that the above-ground plant parts and the root system of control and treated wild-type plants had the same size at the beginning of the experiment. After the same time period as the untreated wild type and mutant lines, plants treated with 1 μM propiconazole were evaluated for gall development (**Fig. 7**). It can be clearly seen that the inhibition of BR synthesis resulted in reduction of gall size and consequently the root system on these plants was larger. Transformed into a disease index (DI; Siemens et al. 2002), the results showed that again this index was lower and more plants were found in disease classes indicative of tolerance (**Fig. 8**). When the percentage of plants in individual disease classes is displayed separately, it is obvious that inhibition of BR synthesis resulted in more plants in lower disease classes, leading to significant ($P < 0.01$) differences between control and treated plants (**Fig. 8**). The DI of Enkheim-2 (En-2) plants in this experimental approach was somewhat lower when compared with that of the following experiment (see below), perhaps due to the treatment with larger amounts of water every second day during the treatment, which might have led to dilution of spores. However, additional treatment of wild-type plants with an active BR did not cause any further increase in gall size (data not shown).

In addition, three mutants in BR signaling were investigated: the receptor mutant *bri1-6*, as well as the suppressor mutants *bri1-5 bak1-1D* and *bri1-5 brs1-1D*. Even though these BR signaling mutant lines are smaller than the wild type (shown for *bri1-6* in **Supplementary Fig. S7**), reduction of gall size was obvious and healthy root tissue was also present for *bri1-6*

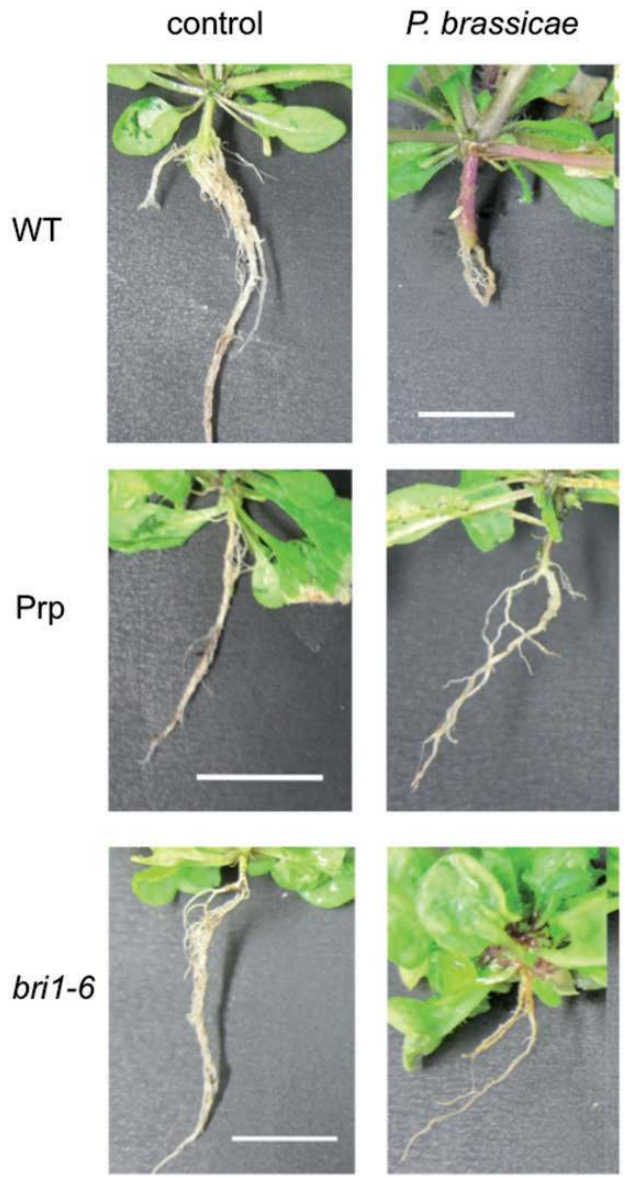

Fig. 7 Gall phenotype of the wild type (En-2), the wild type treated with 1 μM propiconazole and *bri1-6* mutant plants. The left-hand panels show control roots, and the right-hand panels show the roots infected with *P. brassicae*. The scale bar represents 1 cm. For above-ground phenotypes, see **Supplementary Fig. S7**.

(**Fig. 7**). The DI mentioned above also takes into account that smaller plants could produce smaller galls. Using this index, *bri1-6* had a significantly lower DI compared with the respective wild-type En (**Fig. 8**). The result becomes more obvious when the percentage of plants in individual disease classes is displayed, where *bri1-6* had more plants in lower disease classes than the wild type, again showing significant differences ($P < 0.01$) between wild-type and mutant populations (**Fig. 8**). It should be noted that on *bri1-6* plants as well as for wild-type plants treated with the BR synthesis inhibitor propiconazole, the root was not completely transformed into a gall and there were still macroscopically intact roots visible (**Fig. 7**). A variation in the severity of disease symptoms is shown in **Supplementary Fig. S7**. In contrast, all wild-type plants had roots that were completely transformed into galls. Two suppressor mutants for *BRI1* were also included, which had an intermediate phenotype concerning plant size (data not shown). Both (*bri1-5 bak1-1D* and *bri1-5 brs1-1D*) are in the Wassilewskija (WS) background. The DI did not show any difference compared with the wild type (**Fig. 8**), but when the data were displayed again as a percentage of plants in the different disease classes, more plants were found in class 3 for the two mutant lines, whereas the wild type had more in class 4 (**Fig. 8**), even though for the whole data set no significance could be calculated. This would confirm the intermediate phenotype of the suppressor lines for *bri1*.

Discussion

While gene expression patterns using whole tissues have been analyzed at different time points during clubroot disease (Siemens et al. 2006, Agarwal et al. 2011), this report downscales the resolution by investigation of the gene expression profiles of pools of host cells containing different developmental stages of the pathogen isolated by LMPC. In plant–pathogen interactions not many reports of such attempts exist, especially using root tissue. Examples are arbuscular mycorrhiza-colonized roots (Guether et al. 2009, Gaude et al. 2012) and roots colonized with nematodes (Klink et al. 2005, Klink et al. 2009). Here, we report the separation of different developmental stages of the protist, *P. brassicae*, a true intracellular pathogen, causing clubroot disease. Due to its obligate biotrophic lifestyle, the interaction with the host cell is very strong. The time points after inoculation used in this study are similar to those investigated by Siemens et al. (2006) using whole roots, with the exception that in our work resting spores which never matured were visibly present in sections of infected roots. We have compared our results obtained with homogeneous cell type populations with the results from the whole root tissue study. The range of developmental stages of *P. brassicae* in our investigation is defined from host cells containing small plasmodia at 14 and 21 dai close to the central cylinder to strongly hypertrophied host cells containing large plasmodia in the outer cortex of the roots (**Fig. 1A**) also at 14 and 21 dai. The latest stages are large plasmodia in enlarged cells 21 dai, which is close to sporulation. Small and large plasmodia-containing cells were chosen, because the plasmodia represent the main developmental stage within the root cortex. They are involved in reorganization of the host tissue for their benefit and also alter nutritional flow towards the root galls (Ludwig-Müller et al. 2009). The central cylinder was also analyzed during the early time point 14 dai, because young plasmodia have been observed there (Ludwig-Müller et al. 1999). Even though the focus was on BR-related genes, many other metabolic pathways are differentially regulated, which will be briefly discussed.

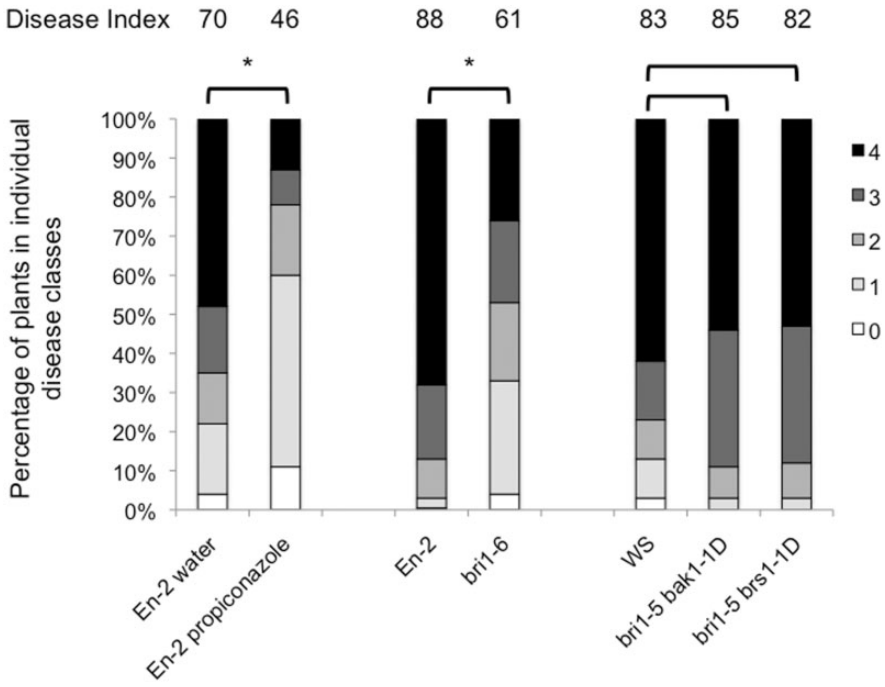

Fig. 8 Phytopathological analysis of BR synthesis inhibition and BR signaling mutants in comparison with wild-type plants 28 dai. The wild type (En-2) was treated with the BR biosynthesis inhibitor propiconazole at 1 μM. The BR signaling mutants tested are *bri1-6* (En-2 background) and two suppressor mutant lines *bri1-5 bak1-1D* and *bri1-5 brs1-1D* (in the WS background). The experiments with En-2 plants are given as a separate data set, because the control groups were treated differently (see the Materials and Methods). The percentage of plants in the individual disease classes is shown. 0, no symptoms; 1, very small galls mainly on lateral roots and that do not impair the main root; 2, small galls covering the main root and few lateral roots; 3, medium to large galls, also including the main root; and 4, severe galls on lateral root, main root or rosette; fine roots completely destroyed. For each treatment, at least 60 Arabidopsis plants per tray were analyzed, and two trays were investigated in one experiment. The experiments were repeated with independently cultivated plant material (double mutants twices, propiconazole treatment three times and *bri1-6* six times). The qualitative disease assessment data were analyzed first by using the Kruskal–Wallis test and subsequently by comparing the mean rank differences. The brackets indicate the two samples which were compared, and an asterisk indicates a significant difference at $P < 0.01$. The disease index for each sample is given as a number above the respective histograms.

Further transcriptional changes should be used as indications for future, more detailed, investigations.

Many metabolic pathways are altered in cells harboring plasmodia

The analysis of the transcriptome in homogeneous cell type populations of the host inoculated with *P. brassicae* provided more detailed information on metabolic processes during reprogramming of host cells and the development of plasmodia at two different time points after inoculation. Both young and, even more so, older growing plasmodia should be regarded as metabolically highly active, which could have an effect on the host cells. It was shown recently that the inhibition of invertase activity in Arabidopsis reduced club size significantly after infection with *P. brassicae* (Siemens et al. 2011), highlighting the importance of assimilates for the pathogen. Major pathways influenced in our investigation were sugar metabolism, lipid synthesis and metabolism, and fermentative processes. In contrast to lipid metabolism, differential gene regulation associated with fermentation did not show up in the whole root array data. While the increase in energy metabolism, for example glycolysis, TCA cycle, electron transport and N/S assimilation, was to be expected, the observation that fermentation-related transcripts increased was somewhat surprising.

A role for fermentation processes in plant–pathogen interactions has been postulated earlier (Wildermuth 2010). In tissues with high O_2 demand, which can be the case in obligate biotrophic pathogen interactions with the host, hypoxia or anoxia is a frequent metabolic status even during normal development, due to a lack of an active transport system for molecular oxygen (Geigenberger 2003). The fermentative pathway could thus be important to maintain the primary energy metabolism of the host cell under conditions of an increased metabolic flux (hexose to pathogen) and an assumed low oxygen pressure (high oxygen for pathogen; oxygen consumption by a hypersensitive reaction) at the site of pathogen infection (Proels et al. 2011). Pathuri et al. (2011) showed that alcohol dehydrogenase 1 of barley modulates susceptibility to the parasitic fungus *Blumeria graminis* f.sp. *hordei*. Furthermore, Tadege et al. (1998) showed that overexpression of a pyruvate decarboxylase in potato leaves results in increased acetaldehyde concentrations and induction of plant defense reactions. In the case of the Arabidopsis–*P. brassicae* interaction, the induction

of fermentation processes in plasmodia-containing cells corroborates the increased energy metabolism, which could also lead to oxygen shortage in this interaction, as explained above.

Furthermore, it was also shown that in cells containing old, large plasmodia, cell wall synthesis tended to be more down-regulated. This has been previously interpreted as reduced defense of the plant (Agarwal et al. 2011), or as a prerequisite for cell enlargement (Ludwig-Müller 2009).

Differential regulation of plant hormone metabolism

Multiple lines of evidence indicate that plant hormones are involved in the growth of clubroots (reviewed in Ludwig-Müller et al. 2009). In general, four growth-promoting hormone classes are described: auxins, cytokinins, gibberellins and BRs. So far auxins (Grsic-Rausch et al. 2000) and cytokinins (Siemens et al. 2006) have been shown to be responsible for hypertrophy and cell divisions in clubroots. Consequently, Arabidopsis plants with altered auxin levels showed reduced gall formation (Grsic-Rausch et al. 2000). Also, with regard to cytokinins it has been reported that overexpression of *CKX1* and *CKX3* resulted in higher resistance to clubroot (Siemens et al. 2006). Indications for a role of gibberellins in clubroot development are scarce. Recent observations indicate that gibberellin synthesis is not needed for the development of clubroot galls in Arabidopsis (Päsold and Ludwig-Müller 2013). In agreement with this, the LMPC microarray analysis revealed no significant differential regulation patterns for gibberellin-associated transcripts (data not shown). Besides the above-mentioned hormones, BRs are also linked to cell division and are implicaed in regulating cell expansion together with auxins (Clouse 2011b).

To date, expression data for hormone-related transcripts were not stage specific, but based on previous results it can be expected that auxins in particular can be linked to hypertrophied cells. An increased auxin content in infected Arabidopsis roots was correlated with an increase in nitrilase transcripts *NIT1* and *NIT2*, and *nit1* mutants showed smaller galls (Grsic-Rausch et al. 2000). *NIT1*/*NIT2* were also up-regulated in a whole root array analysis (Siemens et al. 2006). In the present cell-specific analysis, a high induction of *NIT2* and a somewhat lower induction for an *NIT1* splice variant was found exclusively in strongly hyptertrophied host cells harboring large plasmodia at 14 and 21 dai which were located in the outer root cortex. The stage-specific strong up-regulation of *NIT2* in these large plasmodia-containing cells at both investigated time points (approximatley 90- and 60-fold induction) was significantly different compared with the regulation found in the whole root array. In contrast, no significant induction was found at the first time point of the whole root array and only a 7-fold increase was observed for the second time point (**Supplementary Table S1**). Two pieces of independent experimental evidence verify the expression patterns from the present study on a cellular level. First, the expression pattern of nitrilase found here in cells harboring large plasmodia 21 dai confirms previous immunolocalization work demonstrating that the nitrilase protein localized to cells harboring large and sporulating plasmodia (Grsic-Rausch et al., 2000) and, secondly, Arabidopsis *promoter::GUS* lines for *nitrilase2* also showed the highest staining in large plasmodia-containing cells (Päsold et al. 2010).

Some of the most highly differentially regulated genes involved in auxin homeostasis from the whole root array experiment, the GH3 family of auxin conjugate synthetases (Staswick et al. 2005), were also up-regulated in plasmodia-containing cells according to the LMPC data (**Supplementary Table S1**). Interestingly, genes belonging to the auxin conjugate hydrolase family were up-regulated in the analysis using homogeneous cell type populations, whereas no evidence for the involvement of auxin conjugate hydrolysis was found in the whole root array in Arabidopsis. These results point to a possible dilution of low abundant transcripts, which can only be detected by the more confined LMPC method. In Chinese cabbage, a differential regulation of auxin conjugate hydrolases was demonstrated during clubroot formation (Schuller and Ludwig-Müller 2006).

Many genes encoding proteins involved in the synthesis and metabolism of defense hormones were differentially regulated when analyzed at the level of homogeneous cell type populations. Since the enzymes are encoded by large gene families, the regulation was not completely consistent for all genes within a family (**Supplementary Fig. S5**). However, generally more genes were up-regulated in cells with older, large plasmodia. At earlier time points, the pathogen might be able to suppress host defense mechanisms, so that its own nutrition is guaranteed. This hypothesis is in agreement with the observation that many defense genes were not up-, but even down-regulated in the whole root array (Siemens et al. 2006, Ludwig-Müller 2009). For JA synthesis mostly increased transcript amounts were observed, which was especially strong in 14CC and 14SP samples (**Supplementary Fig. S5**). However, since it was shown that JA can induce nitrilase (Grsic et al. 1999), the increase in JA biosynthesis might have roles additional to defense activation. Salicylic acid metabolism on the other hand was down-regulated, especially in large plasmodia-containing cells 14 dai (data not shown); a down-regulation of the salicylic acid pathway was confirmed for root hair expression data (Agarwal et al. 2011). ET synthesis was up-regulated mainly in infected host cells (21 LP), while during early stages the regulation of ET synthesis was not so prominent. Agarwal et al. (2011) observed that during the very early interaction between *P. brassicae* and root hairs, ET synthesis is down-regulated. However, intact ET signaling is required to restrict gall size (Knaust and Ludwig-Müller 2013).

Brassinosteroid synthesis and signaling are involved in clubroot formation

Hallmarks of the microscopic clubroot phenotype are the enlarged (hypertrophied) cells as well as the increasing

number of cell divisions (Ludwig-Müller et al. 2009). The first indications that BRs might be involved in gall development came from work by Siemens et al. (2002), who showed that mutants in BR synthesis (*det2*) were more tolerant to the clubroot pathogen, even though the plants were very small. A role for BR in clubroot formation has so far been overlooked, because it was not prominent in whole root arrays (Siemens et al. 2006) (**Supplementary Table S3**). While most genes encoding BR biosynthetic enzymes were considerably up-regulated at several stages and time points in the arrays using homogeneous cell type populations, the genes encoding degrading enzymes were either not regulated at all or were down-regulated in these samples (**Fig. 5**; **Supplementary Table S3**). However, it should be noted that *DET2* transcripts were not differentially regulated, even though the mutant displayed an altered phenotype concerning gall formation. It is assumed that all tissues can synthesize BRs, but the *DET2* expression in roots is quite low, as found in public internet resources (i.e. eFP browser, http://bar.utoronto.ca; Winter et al. 2007) and also for clubroots, which may indicate effects of upper plant parts on gall formation. Further evidence for the involvement of BR synthesis was obtained in this study by treatment of plants with the BR synthesis inhibitor propiconazole, which was recently introduced by Hartwig et al. (2012). These authors showed that at low concentrations this compound inhibited the biosynthesis of brassinolide when Arabidopsis plants were grown on agar plates containing the inhibitor. Here we show that this compound also has inhibitory action when plants were grown in soil and the roots were directly treated with the inhibitor dissolved in H_2O. Regular treatment with the biosynthesis inhibitor resulted in a reduction of clubroot symptoms similar to the symptoms observed for the *bri-1-6* receptor mutant (see below).

The LMPC data also revealed differentially regulated genes for BR signaling. The expression of a BR receptor and other genes classified as BR related was up-regulated in cells harboring plasmodia of different size and age, including the central cylinder of infected roots (**Table 2**; **Fig. 6**). This correlates with the reduced gall size of *bri1* mutants (**Figs. 7**, **8**), whereas suppressor mutants (*bri1-5 bak1-1D*, Li et al. 2002; *bri1-5 brs1-1D*, Li et al. 2001) showed an intermediate phenotype, even though *BRS1* was only up-regulated in the central cylinder. Since the mutant allele *bri1-1* (Clouse et al. 1996, Friedrichsen et al. 2000) is extremely dwarfed, and therefore the infection with *P. brassicae* could not be evaluated, the mutant *bri1-6* (Noguchi et al. 1999, Friedrichsen et al. 2000) in the En background was analyzed in comparison with the respective wild type. The *bri1-6* mutant is somewhat smaller than the wild type, but may be three times the size of *bri1-1* (data not shown). By showing that there were still roots attached to the gall system of mutant plants, a function for BRs in clubroot development has herewith been demonstrated.

Auxin–brassinosteroid cross-talk

Stage-specific transcriptional changes of BR-associated genes implied that BRs are specifically important for the development of cell size. BRs could be involved in causing hypertrophy together with auxin, because genes encoding biosynthetic enzymes, for example CPD, regulated by auxin were positively affected in plasmodia-containing cells (**Figs. 5**, **6**). While auxin induces expression of a gene encoding a biosynthetic enzyme involved in BR synthesis via the transcription factor BRX (Beuchat et al. 2010), BR induces transcription factors (ARFs) involved in the activation of auxin-responsive genes (Depuydt and Hardtke 2011), and a set of common target genes for both hormones has been described (Goda et al. 2004). Even though BRX and some ARFs were not obviously differentially regulated in our experiments, interplay between auxin (**Supplementary Tables S1**) and BR signaling is possible and could be responsible for the hypertrophy observed in mature clubroots. A direct point for auxin–BR cross-talk is BIN2, encoding the AtSK protein, a shaggy-like kinase family member. In the BR signaling pathway, BIN2-mediated phosphorylation appears to promote BZR1 export from the nucleus (Ryu et al. 2007). Both BIN2 and the corresponding phosphatase PP2A are up-regulated in many plasmodia-containing cells investigated, which is at first glance contradictory (**Fig. 6**; **Table 2**). However, the role of BIN2 could be to regulate auxin–BR cross-talk, while PP2A only regulates BR signaling. BR signaling triggers the BIN2-mediated phosphorylation of the ARF2 repressor to inhibit its binding to auxin-response elements in the promoters of BR/auxin-regulated genes (Vert et al. 2008). Once this repressor (and also others) is removed, auxin-dependent gene expression via positive ARFs could be activated. Thus, up-regulation of *BIN2* might be involved in positively regulating auxin-related gene expression (**Fig. 6**).

For the regulation of transcription factors it could be that, since the cut-off used to define up- or down-regulation was ± 2, transcription factors with low expression levels did not fit the criteria, even if their presence in the individual cells could contribute to transcriptional activation. It was shown in microarrays that the levels of transcription factors are usually quite low (Czechowski et al. 2004). Another transcriptional regulator of BR synthesis, *CES* (Poppenberger et al. 2011), was even down-regulated in three investigated cell types (**Fig. 6**; **Table 2**), suggesting that direct transcriptional activation might be achieved by different signals, perhaps deriving from *P. brassicae* itself.

Brassinosteroids and xylem formation

In addition to many other growth regulatory effects, BRs are involved in the proper development of the vasculature in stems (Ibanes et al. 2009). Changes in vessel structures were already reported as early as in the 1980s by Ikegami and Yamashita (1983), who described the disorientation of vessels in turnip roots infected with *P. brassicae*. Thus it is no surprise that many genes connected to BR synthesis were also up-regulated in the central cylinder area. Further indications for a role for xylogenesis in gall formation comes from recent work by Malinowski et al. (2012), who showed by quantitiative RT–PCR that the transcription of two NAC-domain-containing transcription

factors, *VND6* and *VND7*, was down-regulated in root galls. These two transcripts were identified as factors involved in BR-related transcription according to TAIR annotations and were consistently down-regulated in 14CC, 14SP, 14LP and 21LP (**Table 2**). It was shown that the reprogramming of the host tissue was dependent on cell division and retention of meristematic activity (Malinowski et al. 2012). In addition, gall development was dependent on the meristematic activity in the vascular cambium, because disrupting this activity resulted in smaller galls. In galls, the proper formation of xylem was altered in favor of enlargement of the meristematic region (Malinowski et al. 2012). BRs may be synthesized by the plant in the central cylinder region in order to counteract the disassembling vasculature, if xylogenesis is repressed, for example by *VND6* and *VND7*.

Brassinosteroids and disease resistance

The above-mentioned findings point to a role for BRs in tissue hypertrophy. Nevertheless, a role for BRs in disease resistance cannot be excluded. Application of brassinolide promotes disease resistance in rice and tobacco (Nakashita et al. 2003). In the context of clubroot disease our data revealed the opposite response: reduction of BR synthesis led to tolerance and treatment with BR did not alter disease symptoms. In a recent investigation it has been shown that BR can act antagonistically or synergistically with responses to MAMPs (microbial-associated molecular patterns) and that the synergistic activities of BRs on MAMP responses require BAK1 (Belkhadir et al. 2012). In addition to BRI1, BAK1 also interacts with the co-receptor FLS2, resulting in the activation of the plant immune response (Wang 2012). On the other hand, BRs also inhibited signaling triggered by the BAK1-independent recognition of the fungal PAMP (pathogen-associated molecular pattern) chitin, and a general mechanism in which BR-mediated growth directly antagonizes innate immune signaling has been proposed (Albrecht et al. 2012). For biotrophic pathogens it has been suggested that they have evolved virulence mechanisms to detect or create physiological states in which BR concentrations are optimal for pathogen success (Belkhadir et al. 2012). However, to characterize the observed tolerance response to clubroot further, the amount of *P. brassicae* after inhibition of the BR biosynthesis and in *bri* mutants would need to be determined.

Conclusion

Taking all the results together, BRs could be functioning in different areas during club development such as cell division and elongation, xylogenesis and plant defense responses. In addition, several differentially regulated genes in various pathways have been identified as being stage specific in infected host cells. Future investigations of these important pathways, such as fermentation, could shed light on their importance for clubroot development. Since it was shown that the clubroot disease caused by *P. brassicae* can be analyzed on the molecular level in a cell- and stage-specific manner, it will be possible to use RNaseq techniques for the analysis of specific transcripts from the pathogen in the future. This might lead to the identification of key regulators for defined developmental stages of *P. brassicae* and also signals involved in triggering the observed changes in the plant's response.

Materials and Methods

Growth conditions and infection procedure

Seeds of *A. thaliana* ecotypes Columbia (Col-0), WS or En were soaked on wet filter paper in a Petri dish at 8°C for 72 h and sown onto a mixture of peat containing compost and sand (volume ratio 5 : 2). Plants were grown in a growth chamber at 24°C with a 12 h daylight period (100 μmol $m^{-2} s^{-1}$) and at 18°C for 12 h in the dark. Air humidity was 60% and the plants were regularly watered with tap water. After 14 d, the plants were inoculated with 2 ml of a resting spore suspension (2×10^6 spores ml^{-1}) of the *P. brassicae* (single spore) isolate 'e_3' as described by Fähling et al. (2003) and Graf et al. (2004). Control plants were watered with the corresponding phosphate buffer only (50 mM KH_2PO_4, pH 5,5 adjusted with 25% K_2HPO_4). *Brassica rapa* L. ssp. *pekinensis* cv. 'Granaat' (ECD-05) was used for propagation of the *P. brassicae* isolate. The spores were isolated as described by Mithen and Magrath (1992). At defined time points, roots were harvested and carefully washed with deionized water. Root material for RNA isolation was instantly frozen in liquid nitrogen whereas root material for paraffin embedding was instantly dissected and fixed as described below.

Treatment with 1 μM propiconazole and 0.1 μM of an active BR (22α,23α-dihydroxy-24β-methyl isomer of brassinolide; Cohen and Meudt 1983, Ludwig-Müller and Cohen 2002) was performed twice a week by pipetting 0.5 ml of the compounds directly onto each plant. Concentrations were chosen according to Hartwig et al. (2012). The controls were likewise treated with H_2O. The treatments were started on the same day that the inoculation with resting spores was done. The inoculation was done first, then the spores were allowed to settle into the soil and the first treatment with chemicals was performed 2 h later. Treatment continued until the final evaluation of disease symptoms 28 dai.

Phytopathological analysis of brassinosteroid mutants

Disease symptoms were examined 28 dai. Disease severity was qualitatively assessed by using the DI described by Siemens et al. (2002). For this parameter, the disease symptoms were categorized using a scale with five classes according to Klewer et al. (2001): 0 (no symptoms); 1 (very small galls mainly on lateral roots and that do not impair the main root); 2 (small galls covering the main root and few lateral roots); 3 (medium to large galls, also including the main root; plant growth might be

impaired); and 4 (severe galls on lateral root, main root or rosette; fine roots completely destroyed; plant growth is reduced). For each treatment, at least 60 Arabidopsis plants per tray were analyzed, and two trays were investigated in one experiment. The experiments were repeated at least once with independently cultivated plant material. The numbers of individual experiments are given in the legend to **Fig. 8**. The percentage of plants in individual disease classes was determined according to Jäschke et al. (2010). The qualitative disease assessment data were analyzed first by using the Kruskal–Wallis test and subsequently by comparing the mean rank differences (Siegel and Castellan 1988).

Tissue fixation and dehydration

Tissue fixation was performed with the HOPE® Reagents (DCS, Innovative Diagnostic Systems). Transverse sections of the main roots of Arabidopsis ($< 5\ mm^3$) were immediately submerged in 1.5 ml of ice-cold (0–4°C) HOPE® I and incubated on ice overnight. All subsequent incubation steps were performed with pre-cooled solutions and were done at 0–4°C. The next day the HOPE® I solution was discarded and staining of the tissue was performed in 85% ethanol with a few crystals of eosin (Eosin Y disodium salt, Sigma) for 30 min (the eosin staining facilitated the recovery of the tissue within the cured paraffin wax blocks). After removal of the staining solution, dehydration started with incubation in a pre-mixed HOPE® II/acetone solution [1.5 ml of acetone (100%) + 1.5 µl of HOPE® II] for 2 h. After the HOPE® II/acetone solution was discarded, the tissue was incubated in ice-cold pure acetone for 3 h, replacing the acetone during this incubation step several times. Next, acetone was replaced by pre-warmed low-melting paraffin (52–54°C) (DCS, Innovative Diagnostic Systems) and the tissue was incubated at 60°C for 1 h. In the next step, this paraffin wax was replaced by Paraplast X-Tra (Carl Roth GmbH) and kept at 60°C for 1 h while replacing the paraffin either once or twice. Then the paraffin wax including the tissue was poured in a mold and, using pre-warmed needles, the tissue was placed in the desired position at 60°C. The paraffin wax was cooled down for hardening at room temperature. The embedded tissue was stored until further use at 8°C with silica gel as desiccant.

Sectioning, slide preparation and quality control

Every surface of the microtome as well as every instrument that came in contact with the sections (e.g. blade, tweezers, etc.) was cleaned with RNaseZAP® (Sigma-Aldrich Chemie GmbH). The paraffin wax block was clamped directly in the 'sample holder' of the microtome and sections of 12–20 µm were cut, taken off with tweezers and placed on a drop of 75% ethanol pipetted on a PEN-slide (PALM MembraneSlides PEN/NF, Carl Zeiss MicroImaging GmbH). The PEN-slides were placed on a heating plate at 45°C and incubated until the sections became stretched. Excess ethanol was poured off and the samples were air-dried at room temperature. A better attachment of the sections onto the PEN-slides was achieved by placing the slides for a few seconds on a heating plate at 60°C until the paraffin started to melt. PEN-slides with mounted sections were stored at 8°C with silica gel as desiccant until LMPC. Before LMPC, the RNA quality of the embedded plant material was determined by isolating total RNA from the paraffin sections with an ArrayPure™ Nano-scale RNA Purification Kit (Epicentre Biotechnologies), whereas removal of paraffin wax was done as follows: 20 µm sections of paraffin-embedded tissue were incubated in a reaction tube in 1.5 ml of xylene at room temperature for 10 min. Solvent was poured off and treatment repeated. The tissue was then incubated twice in 1 ml of 100% ethanol at room temperature for 10 min. All remaining ethanol was aspirated and the tissue lysed in Nano-scale Lysis Solution containing proteinase K according to the manufacturer's instructions. Isolated RNA was quantified with an ND-1000 Spectrophotometer (NanoDrop Technologies, Inc.) and the integrity of the RNA was checked with the Agilent 2100 Bioanalyzer platform using the RNA 6000 Pico Kit (Agilent Technologies Manufacturing GmbH & Co. KG).

Laser microdissection and pressure catapulting and sample processing for microarray hybridization

Before cells have been collected with LMPC, paraffin wax was removed by incubation of PEN-slides with tissue sections in fresh xylene for 5–10 min. Slides were then air-dried under a fume hood for a few minutes and mounted on the PALM® MicroBeam system. Cells and tissue areas of interest were selected with the PALM® RoboSoftware, microdissected and catapulted into the cap of a collection device (PALM AdhesiveCaps, Carl Zeiss MicroImaging GmbH) located on top of the desired area. For every sample, 200–300 cells were collected. For each type of sample, the laser focus adjustment was performed individually. For cutting and catapulting, the menu 'RoboLPC' was used, with laser power 85–100, laser focus 74–79. Cells were lysed directly in the cap of the collection device using 6.4 µl of SuperAmp Lysis Buffer (Miltenyi Biotec) according to the manufacturer's instruction and stored at −20°C.

Superamplification, labeling and DNA microarray hybridization and analysis of gene expression were performed at the Miltenyi Biotec gene array facility (Bergisch Gladbach, Germany), using Agilent technology (Agilent Technologies). The SuperAmp™ Technology method has been successfully applied in previous research (e.g. Appay et al. 2007). For the generation of amplified cDNA (SuperAmp Service, Miltenyi Biotec), the mRNA was extracted from the RNA samples using magnetic beads and transcribed into cDNA using tagged random and oligo(dT) primer. First-strand cDNA was 5′ tagged using 8 U of terminal deoxynucleotidyl transferase (Fermentas) and incubated for 60 min at 37°C, 35 min at 22°C before heat inactivating at 70°C for 5 min. Tagged cDNA was globally amplified (Expand Long Template PCR

System DNA Pol Mix, Roche) using primer complementary to the tag sequence and incubation at 78°C for 30 s, 20 cycles of 94°C for 15 s, 65°C for 30 s and 68°C for 2 min, followed by 21 cycles of 94°C for 15 s, 65°C for 30 s and 68°C for 2.5 min with an extension of 10 s per cycle and a final step of 68°C for 10 min. The PCR product was purified (NucleoSpin® Extract II, Macherey-Nagel) and the cDNA yield measured. The average length of superamplified cDNA products ranged between 200 and 1,000 bp. The results of the Bioanalyzer run were visualized in a gel imager and an electropherogram using the Agilent 2100 Bioanalyzer expert software. Labeling of 250 ng of purified PCR product was done with Cy3-dCTP (Amersham) in a Klenow fragment (10 U) reaction for 1 h 50 min at 37°C before inactivating through addition of 5 µl of 0.5 M EDTA pH 8.0. Finally, 1.25 µg of Cy3-labeled and purified (CyScribe GFX Purification Kit, GE Healthcare) cDNAs in hybridization buffer were hybridized overnight (17 h, 65°C) to the 4×44K Agilent Arabidopsis Oligo 3 Microarray (Agilent Technologies) using Agilent's recommended hybridization chamber and oven. Microarrays were washed once with 6× SSPE buffer containing 0.005% *N*-lauroylsarcosine for 1 min followed by a second wash with 0.06× SSPE containing 0.005% *N*-lauroylsarcosine for 1 min and a final wash step with acetonitrile for 30 s. All washing steps were performed at room temperature.

Fluorescence signals of the hybridized Agilent Microarrays were detected using Agilent's Microarray Scanner System (Agilent Technologies). Microarray data analysis was performed using Resolver (Rosetta Biosoftware) and MEV (TIGR) software.

Microarray data accession number

The microarray data determined in this study can be downloaded from the Genome expression Omnibus database (http://www.ncbi.nlm.nih.gov/geo) under the accession number GSE44676.

RT–PCR in initial experiments

Total RNA was isolated from infected roots of *A. thaliana* ecotype Col-0 at different time points of infection (15, 20, 26 and 34 d after infection) and from control roots at 34 d after infection using the TRIzol® method (Invitrogen Life Technologies) for carbohydrate-enriched tissue. Since different developmental stages of the pathogen are present in total root tissues, a mixture of the isolated RNA samples has been used for the further analysis of *P. brassicae* actin expression. Total RNA of two paraffin cross-sections of infected roots at 24 dai was isolated with an ArrayPure™ Nano-scale RNA Purification Kit (Epicentre Biotechnologies), and total RNA purification of the LMPC samples (250–300 cells), isolated from infected roots at 24 dai and control roots, was performed with an RNeasy® Micro Kit (Qiagen) according to the manufacturer's instructions. Residual genomic DNA from complete infected and control roots was removed by digestion with Turbo DNA-free™ (Ambion) according to the manufacturer's protocol. In these samples, first-strand cDNA synthesis was performed with 5 µg of DNase-digested total RNA, 0.8 µM oligo dT (15) deg primers (MWG Biotech), 0.4 mM dNTPs, 1 × first strand buffer (Invitrogen), 20 mM dithiothreitol (DTT; Invitrogen), 40 U of RNaseOUT™ (Invitrogen) and 400 U of M-MLV Reverse Transcriptase (Invitrogen) for 50 min at 37°C. The reaction was terminated by incubation at 70°C for 15 min. Digestion of genomic DNA and cDNA synthesis of the isolated RNA from paraffin-embedded sections and LMPC samples has been performed with a SuperScript® III Platinum® CellsDirect Two-Step qRT-PCR Kit (Invitrogen) according to the manufacturer's protocol. PCR was performed with 0.2 mM dNTPs (Invitrogen Life Technologies), 3 mM $MgCl_2$ (Invitrogen Life Technologies), 0.5 µM forward and reverse primer, and 1 U of Platinum® Taq DNA Polymerase (Invitrogen Life Technologies), in a total volume of 20 µl. The PCR amplification protocol consisted of a denaturation cycle at 95°C for 3 min, continued with 46 cycles of 30 s at 95°C, 30 s at 55°C and 45 s at 72°C; final extension was done at 72°C for 5 min. The following primers (synthesized by Eurogentec) were used for detection of *P. brassicae*: Pb-act1, 5′-ATG TCC AAC TCG GAG CAG TC-3′; and Pb-act2, 5′-GGA CTC GTT GCC GAT CAT-3′.

Quantitative RT-PCR

All primers for quantitative RT–PCR were synthesized by Eurogentec. Sequences of all primers for quantitative RT–PCR are listed in **Supplementary Table S5**. Before running the quantitative RT–PCR experiments, the optimal primer concentration for each primer pair and the PCR efficiency were determined. Quantitative RT–PCR analysis was performed under the following conditions: RealMasterMix-Sybr ROX (5 PRIME GmbH), primer mix (0.25–0.4 µM each) and 1 µl of cDNA from LMPC-sampled cells using the Mastercycler ep realplex gradient S (Eppendorf AG). Reactions consisting of a total volume of 20 µl were run in triplicate in a 96-well thin-walled PCR plate (Thermo Scientific). The PCR amplification protocol consisted of a denaturation cycle at 95°C for 2 min, continued with 50 cycles of 20 s at 95°C, 15 s at 61°C and 20 s at 68°C. For verification of PCR products, each amplification reaction was checked for the presence of non-specific products by melting curve analysis (60–95°C). For selected primer pairs, quantitative RT–PCR experiments were repeated.

Expression levels for each target gene were relatively quantified following normalization to EMB1075 (AT1G43710), an endogenous reference gene which was unregulated in all samples, and correlated to the negative control (uninfected root at a given time point). The final calculation was carried out by the arithmetic formula 2^{-DDCP} (Pfaffl 2001) calculated by the REST analysis.

Analysis software/tools

To obtain a more general overview of gene expression changes, analysis using MapMan (Thimm et al. 2004) was conducted. Ratios of control to infected roots were calculated for each time point for all values, and the values were converted to log2 in

Microsoft Excel files before they were imported in the MapMan software. Further analysis was performed using the GO terms in PageMan (Usadel et al. 2005).

The metabolic pathways for hormone synthesis were analyzed using AraCyc (available from The Arabidopsis Information Resource Website, http://www.arabidopsis.org/tools/aracyc). The AraCyc database for Arabidopsis Col-0 was used for running the expression viewer tool at each time point. Up- or down-regulation of genes is displayed in a color relative to the expression levels.

The annotation of the transcripts presented in the tables was performed using the AGI numbers from the TAIR (http://www.arabidopsis.org/) database. Annotated genes related to auxin/cytokinin were taken from Siemens et al. (2006).

Supplementary data

Supplementary data are available at PCP online.

Funding

This work was supported by the Saxonian Ministery for Environment and Geology (LfULG); the Gesellschaft der Freunde und Förderer (GFF) der Technischen Universität Dresden.

Disclosures

The authors have no conflicts of interest to declare.

Acknowledgments

The BR analog (22α,23α-dihydroxy-24β-methyl isomer of brassinolide) was a gift of Dr. Jerry D. Cohen, University of Minnesota, USA. We thank Silvia Heinze (Technische Universität Dresden) for technical assistance.

References

Agarwal, A., Kaul, V., Faggian, R., Rookes, J.E., Ludwig-Müller, J. and Cahill, D.M. (2011) Analysis of global host gene expression during the primary phase of the *Arabidopsis thaliana–Plasmodiophora brassicae* interaction. *Funct. Plant. Biol.* 38: 462–478.

Albrecht, C., Boutrot, F., Segonzac, C., Schwessinger, B., Gimenez-Ibanze, S., Chinchilla, D. et al. (2012) Brassinosteroids inhibit pathogen-associated molecular pattern-triggered immune signaling independent of the receptor kinase BAK1. *Proc. Natl Acad. Sci. USA* 109: 303–308.

Alix, K., Lariagon, C., Delourme, R. and Manzanares-Dauleux, M.J. (2007) Exploiting natural genetic diversity and mutant resources of *Arabidopsis thaliana* to study the *A. thaliana–Plasmodiophora brassicae* interaction. *Plant Breed.* 126: 218–221.

Appay, V., Bosio, A., Lokan, S., Wiencek, Y., Biervert, C., Küsters, D. et al. (2007) Sensitive gene expression profiling of human T cell subsets reveals parallel post-thymic differentiation for $CD4^+$ and $CD8^+$ lineages. *J. Immunol.* 179: 7406–7414.

Belkhadir, Y., Jaillas, Y., Epple, P., Balsemao-Pires., Dangl, J.D. and Chory, J. (2012) Brassinosteroids modulate the efficiency of plant immune responses to microbe-associated molecular patterns. *Proc. Natl Acad. Sci. USA* 107: 460–465.

Beuchat, J., Scacchi, E., Tarkowska, D., Ragni, L., Strnad, M. and Hardtke, C.S. (2010) BRX promotes Arabidopsis shoot growth. *New Phytol.* 188: 23–29.

Bruder, E.D., Lee, J.J., Widmaier, E.P. and Raff, H. (2007) Microarray and real-time PCR analysis of adrenal gland gene expression in the 7-day-old rat: effects of hypoxia from birth. *Physiol. Genomics* 29: 193–200.

Cao, T., Tewari, J. and Strelkov, S.E. (2007) Molecular detection of *Plasmodiophora brassicae*, causal agent of clubroot of crucifers, in plant and soil. *Plant Dis.* 91: 80–87.

Chandran, D., Inada, N., Hather, G., Kleindt, C.K. and Wildermuth, M.C. (2010) Laser microdissection of Arabidopsis cells at the powdery mildew infection site reveals site-specific processes and regulators. *Proc. Natl Acad. Sci. USA* 107: 460–465.

Clouse, S.D. (2011a) Brassinosteroid signal transduction: from receptor kinase activation to transcriptional networks regulating plant development. *Plant Cell* 23: 1219–1230.

Clouse, S.D. (2011b) Brassinosteroids. *The Arabidopsis Book* e0151. doi: 10.1199/tab.0151.

Clouse, S.D., Langford, M. and McMorris, T.C. (1996) A brassinosteroid-insensitive mutant in Arabidopsis thaliana exhibits multiple defects in growth and development. *Plant Physiol.* 111: 671–678.

Cohen, J.D. and Meudt, W.J. (1983) Investigations on the mechanism of the brassinosteroid response. I. Indole-3-acetic acid metabolism and transport. *Plant Physiol.* 72: 691–694.

Czechowski, T., Bari, R.P., Stitt, M., Scheible, W.-R. and Udvardi, M.K. (2004) Real-time RT–PCR profiling of over 1400 Arabidopsis transcription factors: unprecedented sensitivity reveals novel root- and shoot-specific genes. *Plant J.* 38: 366–379.

Deeken, R., Ache, P., Kajahn, I., Klinkenberg, J., Bringmann, G. and Hedrich, R. (2008) Identification of *Arabidopsis thaliana* phloem RNAs provides a search criterion for phloem-based transcripts hidden in complex datasets of microarray experiments. *Plant J.* 55: 746–759.

Depuydt, S. and Hardtke, C.S. (2011) Hormone signalling crosstalk in plant growth regulation. *Curr. Biol.* 21: R365–R373.

Devos, S., Vissenberg, K., Verbelen, J.-P. and Prinsen, E. (2005) Infection of Chinese cabbage by *Plasmodiophora brassicae* leads to a stimulation of plant growth: impacts on cell wall metabolism and hormonal balance. *New Phytol.* 166: 241–250.

Fähling, M., Graf, H. and Siemens, J. (2003) Pathotype-separation of *Plasmodiophora brassicae* by the host plant. *J. Phytopathol.* 151: 425–430.

Friedrichsen, D.M., Joazeiro, C.A., Li, J., Hunter, T. and Chory, J. (2000) Brassinosteroid-insensitive-1 is a ubiquitously expressed leucine-rich repeat receptor serine/threonine kinase. *Plant Physiol.* 123: 1247–1256.

Fujioka, S. and Yokota, T. (2003) Biosynthesis and metabolism of brassinosteroids. *Annu. Rev. Plant Biol.* 54: 137–164.

Gaude, N., Bortfeld, S., Duensing, N., Lohse, M. and Krajinski, F. (2012) Arbuscule-containing and non-colonized cortical cells of mycorrhizal roots undergo extensive and specific reprogramming during arbuscular mycorrhizal development. *Plant J.* 69: 510–528.

Geigenberger, P. (2003) Response of plant metabolism to too little oxygen. *Curr. Opin. Plant Biol.* 6: 247–256.

Goda, H., Sawa, S., Asami, T., Fujioka, S., Shimada, Y. and Yoshida, S. (2004) Comprehensive comparison of auxin-regulated and brassinosteroid-regulated genes in Arabidopsis. *Plant Physiol.* 134: 1555–1573.

Graf, H., Fähling, M. and Siemens, J. (2004) Chromosome polymorphism of the obligate biotrophic parasite *Plasmodiophora brassicae*. *J. Phytopathol.* 152: 86–91.

Grsic, S., Kirchheim, B., Pieper, K., Fritsch, M., Hilgenberg, W. and Ludwig-Müller, J. (1999) Induction of auxin biosynthetic enzymes by jasmonic acid and in clubroot diseased Chinese cabbage plants. *Physiol. Plant.* 105: 521–531.

Grsic-Rausch, S., Kobelt, P., Siemens, J., Bischoff, M. and Ludwig-Müller, J. (2000) Expression and localization of nitrilase during symptom development of the clubroot disease in *Arabidopsis thaliana*. *Plant Physiol.* 122: 369–378.

Guether, M., Balestrini, R., Hannah, M., He, J., Udvardi, M.K. and Bonfante, P. (2009) Genome-wide reprogramming of regulatory networks, transport, cell wall and membrane biogenesis during arbuscular mycorrhizal symbiosis in *Lotus japonicus*. *New Phytol.* 182: 200–212.

Halliday, K.J. (2004) Plant hormones: the interplay of brassinosteroids and auxin. *Curr. Biol.* 14: R1008–R1010.

Hartwig, T., Corvalan, C., Best, N.B., Budka, J.S., Zhu, J.-Y., Choe, S. et al. (2012) Propiconazole is a specific and accessible brassinosteroid (BR) biosynthesis inhibitor for Arabidopsis and maize. *PLoS One* 7: e36625.

Ibanes, M., Fabregas, N., Chory, J. and Cano-Delgado, A.I. (2009) Brassinosteroid signaling and auxin transport are required to establish the periodic pattern of *Arabidopsis* shoot vascular bundles. *Proc. Natl Acad. Sci. USA* 106: 13630–13635.

Ikegami, H., Naiki, T., Ito, T. and Imuro, Y. (1982) Ultrastructural growth process of *Plasmodiophora brassicae* in infected cells of Chinese cabbage and turnip. *Res. Bull. Fac. Agr. Gifu Univ.* 46: 9–19.

Ikegami, H. and Yamashita, Y. (1983) Changes of vessel structure in turnip roots infected with *Plasmodiophora brassicae*. *Res. Bull. Fac. Agr. Gifu Univ.* 48: 27–35.

Jäschke, D., Dugassa-Gobena, D., Karlovsky, P., Vidal, S. and Ludwig-Müller, J. (2010) Suppression of clubroot development in *Arabidopsis thaliana* by the endophytic fungus *Acremonium alternatum*. *Plant Pathol.* 59: 100–111.

Kageyama, K. and Asano, T. (2009) Life cycle of *Plasmodiophora brassicae*. *J. Plant Growth Regul.* 28: 203–211.

Klewer, A., Luerßen, H., Graf, H. and Siemens, J. (2001) Restriction fragment length polymorphism markers to characterize *Plasmodiophora brassicae* single-spore isolates with different virulence patterns. *J. Phytopathol.* 149: 121–127.

Klink, V.P., Alkharouf, N., MacDonald, M. and Matthews, B. (2005) Laser capture microdissection (LCM) and expression analyses of *Glycine max* (soybean) syncytium containing root regions formed by the plant pathogen *Heterodera glycines* (soybean cyst nematode). *Plant Mol. Biol.* 59: 965–979.

Klink, V.P., Hosseini, P., Matsye, P., Alkharouf, N.W. and Matthews, B.F. (2009) A gene expression analysis of syncytia laser microdissected from the roots of the *Glycine max* (soybean) genotype PI 548402 (Peking) undergoing a resistant reaction after infection by *Heterodera glycines* (soybean cyst nematode). *Plant Mol. Biol.* 71: 525–567.

Knaust, A. and Ludwig-Müller, J. (2013) The ethylene signaling pathway is needed to restrict root gall growth in Arabidopsis after infection with the obligate biotrophic protist *Plasmodiophora brassicae*. *J. Plant Growth Regul.* 32: 9–21.

Kobelt, P. (2000) Die Verbreitung von sekundären Plasmodien von *Plasmodiophora brassicae* (Wor.) im Wurzelgewebe von *Arabidopsis thaliana* nach immunhistologischer Markierung des plasmodialen Zytoskeletts. Dissertation, Institut für Angewandte Genetik, Freie Universität Berlin, Germany.

Li, J.M., Biswas, M.G., Chao, A., Russell, D.W. and Chory, J. (1997) Conservation of function between mammalian and plant steroid 5-alpha reductases. *Proc. Natl Acad. Sci. USA* 94: 3554–3559.

Li, J., Lease, K.A., Tax, F.E. and Walker, J.C. (2001) BRS1, a serine carboxypeptidase, regulates BRI1 signaling in *Arabidopsis thaliana*. *Proc. Natl Acad. Sci. USA* 98: 5916–5921.

Li, J., Wen, J., Lease, K.A., Doke, J.T., Tax, F.E. and Walker, J.C. (2002) BAK1, an *Arabidopsis* LRR receptor-like protein kinase, interacts with BRI1 and modulates brassinosteroid signaling. *Cell* 110: 213–222.

Ludwig-Müller, J. (2009) Plant defence—what can we learn from clubroots? *Aust. Plant Pathol.* 38: 318–324.

Ludwig-Müller, J. and Cohen, J.D. (2002) Identification and quantification of three active auxins in different tissues of *Tropaeolum majus*. *Physiol. Plant.* 115: 320–329.

Ludwig-Müller, J., Ihmig, S., Bennett, R., Kiddle, G., Ruppel, M. and Hilgenberg, W. (1999) The host range of *Plasmodiophora brassicae* and its relationship to endogenous glucosinolate content. *New Phytol.* 141: 443–458.

Ludwig-Müller, J., Prinsen, E., Rolfe, S. and Scholes, J. (2009) Metabolism and plant hormone action during the clubroot disease. *J. Plant Growth Regul.* 28: 229–244.

Ludwig-Müller, J. and Schuller, A. (2008) What can we learn from clubroots: alterations in host roots and hormone homeostasis caused by *Plasmodiophora brassicae*. *Eur. J. Plant Pathol.* 121: 291–302.

Malinowski, R., Smith, J.A., Fleming, A.J., Scholes, J.D. and Rolfe, S.A. (2012) Gall formation in clubroot-infected Arabidopsis results from an increase in existing meristematic activities of the host but is not essential for the completion of the pathogen life cycle. *Plant J.* 71: 226–238.

Mithen, R. and Magrath, R. (1992) A contribution to the life history of *Plasmodiophora brassicae*: secondary plasmodia development in root galls of *Arabidopsis thaliana*. *Mycol. Res.* 96: 877–885.

Morey, J.S., Ryan, J.C. and Van Dolah, F.M. (2006) Microarray validation: factors influencing correlation between oligonucleotide microarrays and real-time PCR. *Biol. Proced. Online* 8: 175–193.

Nakashita, H., Yasuda, M., Nitta, T., Asami, T., Fujioka, S., Arai, Y. et al. (2003) Brassinosteroid functions in a broad range of disease resistance in tobacco and rice. *Plant J.* 33: 887–898.

Noguchi, T., Fujioka, S., Choe, S., Takatsuto, S., Yoshida, S., Yuan, H. et al. (1999) Brassinosteroid-insensitive dwarf mutants of Arabidopsis accumulate brassinosteroids. *Plant Physiol.* 121: 743–752.

Päsold, S. and Ludwig-Müller, J. (2013) Clubroot (*Plasmodiophora brassicae*) formation in Arabidopsis is reduced after treatment with prohexadione-calcium, an inhibitor for oxoglutaric acid-dependent dioxygenases. *Plant Pathol.* 62: 1357–1365.

Päsold, S., Siegel, I., Seidel, C. and Ludwig-Müller, J. (2010) Flavonoid accumulation in *Arabidopsis thaliana* root galls caused by the obligate biotrophic pathogen *Plasmodiophora brassicae*. *Mol Plant Pathol.* 11: 545–562.

Pathuri, I.P., Reitberger, I.E., Hückelhoven, R. and Proels, R.K. (2011) Alcohol dehydrogenase 1 of barley modulates susceptibility to the

parasitic fungus *Blumeria graminis* f.sp. *hordei*. *J. Exp. Bot.* 62: 3449–3457.

Pfaffl, M.W. (2001) A new mathematical model for relative quantification in real-time RT–PCR. *Nucleic Acids Res.* 29: 2002–2007.

Poppenberger, B., Rozhon, W., Khan, M., Husar, S., Adam, G., Luschnig, C. et al. (2011) CESTA, a positive regulator of brassinosteroid biosynthesis. *EMBO J.* 30: 1149–1161.

Proels, R.K., Westermeier, W. and Hückelhoven, R. (2011) Infection of barley with the parasitic fungus *Blumeria graminis* f.sp. *hordei* results in the induction of *HvADH1* and *HvADH2*. *Plant Signal. Behav.* 6: 1584–1587.

Ryu, H., Kim, K., Cho, H., Park, J., Choe, S. and Hwang, I. (2007) Nucleocytoplasmic shuttling of BZR1 mediated by phosphorylation is essential in *Arabidopsis* brassinosteroid signaling. *Plant Cell* 19: 2749–2762.

Schuller, A. and Ludwig-Müller, J. (2006) A family of auxin conjugate hydrolases from *Brassica rapa*: characterization and expression during clubroot disease. *New Phytol.* 171: 145–158.

Siegel, S. and Castellan, N.J. (1988) Nonparametric Statistics for the Behavioral Sciences. McGraw-Hill, New York.

Siemens, J., Gonzales, M.-C., Wolf, S., Hofmann, C., Greiner, S., Du, Y. et al. (2011) Extracellular invertase is involved in the regulation of the clubroot disease in *Arabidopsis thaliana*. *Mol. Plant Pathol.* 12: 247–262.

Siemens, J., Keller, I., Sarx, J., Kunz, S., Schuller, A., Nagel, W. et al. (2006) Transcriptome analysis of *Arabidopsis* clubroots indicate a key role for cytokinins in disease development. *Mol. Plant-Microbe Interact.* 19: 480–494.

Siemens, J., Nagel, M., Ludwig-Müller, J. and Sacristán, M.D. (2002) The interaction of *Plasmodiophora brassicae* and *Arabidopsis thaliana*: parameters for disease quantification and screening of mutant lines. *J. Phytopathol.* 150: 592–605.

Staswick, P.E., Serban, B., Rowe, M., Tiryaki, I., Maldonado, M.T., Maldonado, M.C. et al. (2005) Characterization of an Arabidopsis enzyme family that conjugates amino acids to indole-3-acetic acid. *Plant Cell* 17: 616–627.

Szakasits, D., Heinen, P., Wieczorek, K., Hofmann, J., Wagner, F., Kreil, D.P. et al. (2009) The transcriptome of syncytia induced by the cyst nematode *Heterodera schachtii* in Arabidopsis roots. *Plant J.* 57: 771–784.

Tadege, M., Bucher, M., Stähli, W., Suter, M., Dupuis, I. and Kuhlemeier, C. (1998) Activation of plant defense responses and sugar efflux by expression of pyruvate decarboxylase in potatoe leaves. *Plant J.* 16: 661–671.

Thimm, O., Blaesing, O., Gibon, Y., Nagel, A., Meyer, S., Krueger, P. et al. (2004) MAPMAN: a user-driven tool to display genomics data sets onto diagrams of metabolic pathways and other biological processes. *Plant J.* 37: 914–939.

Thome, M., Skrablin, M.D. and Brandt, S.P. (2006) Tissue-specific mechanical microdissection of higher plants. *Physiol. Plant.* 128: 383–390.

Usadel, B., Nagel, A., Thimm, O., Redestig, H., Blaesing, O.E., Palacios-Rojas, N. et al. (2005) Extension of the visualization tool MapMan to allow statistical analysis of arrays, display of corresponding genes, and comparison with known responses. *Plant Physiol.* 138: 1195–1204.

Vert, G., Walcher, C.L., Chory, J. and Nemhauser, J.L. (2008) Integration of auxin and brassinosteroid pathways by Auxin Response Factor 2. *Proc. Natl Acad. Sci. USA* 105: 9829–9834.

Wang, Z.-Y. (2012) Brassinosteroids modulate plant immunity at multiple levels. *Proc. Natl Acad. Sci. USA* 109: 7–8.

Wildermuth, M.C. (2010) Modulation of host nuclear ploidy: a common plant biotroph mechanism. *Curr. Opin. Plant Biol.* 13: 1–10.

Winter, D., Vinegar, B., Nahal, H., Ammar, R. and Wilson, G.V. (2007) An 'Electronic Fluorescent Pictograph' browser for exploring and analyzing large-scale biological data sets. *PLoS One* 2: e718.

Ye, H., Li, L. and Yin, Y. (2011) Recent advances in the regulation of brassinosteroid signaling and biosynthesis pathways. *J. Integr. Plant Biol.* 53: 455–468.